7722–7741 *Nucleic Acids Research, 2016, Vol. 44, No. 16* *Published online 2 June 2016*
doi: 10.1093/nar/gkw506

The Pch2 AAA+ ATPase promotes phosphorylation of the Hop1 meiotic checkpoint adaptor in response to synaptonemal complex defects

Esther Herruzo, David Ontoso, Sara González-Arranz, Santiago Cavero, Ana Lechuga and Pedro A. San-Segundo*

Instituto de Biología Funcional y Genómica. Consejo Superior de Investigaciones Científicas and University of Salamanca, 37007 Salamanca, Spain

Received December 22, 2015; Revised May 13, 2016; Accepted May 26, 2016

ABSTRACT

Meiotic cells possess surveillance mechanisms that monitor critical events such as recombination and chromosome synapsis. Meiotic defects resulting from the absence of the synaptonemal complex component Zip1 activate a meiosis-specific checkpoint network resulting in delayed or arrested meiotic progression. Pch2 is an evolutionarily conserved AAA+ ATPase required for the checkpoint-induced meiotic block in the *zip1* mutant, where Pch2 is only detectable at the ribosomal DNA array (nucleolus). We describe here that high levels of the Hop1 protein, a checkpoint adaptor that localizes to chromosome axes, suppress the checkpoint defect of a *zip1 pch2* mutant restoring Mek1 activity and meiotic cell cycle delay. We demonstrate that the critical role of Pch2 in this synapsis checkpoint is to sustain Mec1-dependent phosphorylation of Hop1 at threonine 318. We also show that the ATPase activity of Pch2 is essential for its checkpoint function and that ATP binding to Pch2 is required for its localization. Previous work has shown that Pch2 negatively regulates Hop1 chromosome abundance during unchallenged meiosis. Based on our results, we propose that, under checkpoint-inducing conditions, Pch2 also possesses a positive action on Hop1 promoting its phosphorylation and its proper distribution on unsynapsed chromosome axes.

INTRODUCTION

During meiosis, accurate distribution of chromosomes to the gametes is ensured by the action of meiosis-specific surveillance mechanisms commonly known as the meiotic recombination checkpoint or pachytene checkpoint (1,2) and, more recently, broadly referred to as the meiotic checkpoint network (3). This checkpoint monitors those meiotic events, such as chromosome synapsis and meiotic recombination, which are important to establish the adequate number and distribution of interhomolog connections essential for proper chromosome segregation. The meiotic checkpoint network reinforces the adequate order of events during normal meiotic prophase and, in addition, it is crucial to react to meiotic failures. In response to defects in synapsis and/or recombination, the pachytene checkpoint blocks or delays entry into meiosis I, thus preventing the formation of gametes harboring aneuploidy and other kinds of genetic abnormalities.

Chromosome synapsis is mediated by the synaptonemal complex (SC), an evolutionarily-conserved tripartite structure that holds homologous chromosomes together during the pachytene stage of meiotic prophase I. Meiotic recombination initiates with the generation of programmed DNA double-strand breaks (DSBs), which undergo strictly regulated repair during prophase, preferentially with a non-sister chromatid (4). A fraction of DSBs are repaired to yield crossovers that, together with sister chromatid cohesion, give rise to physical links between homologs – chiasmata– promoting proper chromosome distribution. In some organisms, including budding yeast and mouse, chromosome synapsis is tightly linked to and depends on meiotic recombination.

In *Saccharomyces cerevisiae*, the coiled-coil Zip1 protein is the major component of the central region of the SC. Mutants lacking Zip1 fail to synapse and undergo pachytene checkpoint-dependent meiotic arrest or delay in prophase (5). Importantly, the Red1 and Hop1 structural components of the SC lateral elements (LEs) are also involved in the checkpoint; they function as adaptors to support

*To whom correspondence should be addressed. Tel: +34 923294902; Fax: +34 923224876; Email: pedross@usal.es
Present addresses:
David Ontoso, Molecular Biology Program, Memorial Sloan Kettering Cancer Center, New York, NY 10065, USA.
Santiago Cavero, Department of Experimental and Health Sciences, Pompeu Fabra University, 08003 Barcelona, Spain.

activation of the meiosis-specific Mek1 effector kinase. In particular, phosphorylation of Hop1 at Thr318 by the upstream sensor kinases Mec1/Tel1 is necessary for Mek1 activation by phosphorylation (6,7). Full Mek1 activation involves sequential phosphorylation events that can be genetically separated and biochemically differentiated in phos-tag gels (8). Mec1/Tel1 dependent phosphorylation of Mek1 is followed by *in-trans* autophosphorylation at particular sites in its activation loop (Thr327 and Thr331) (9). Active Mek1 promotes two major meiotic responses: it reinforces interhomolog (IH) recombination bias (10,11), at least in part, through the inhibitory phosphorylation of Rad54 at Thr132 (12) and, on the other hand, it prevents exit from prophase and entry into meiosis I. Several crucial cell-cycle regulators, such as Swe1, Ndt80 and Cdc5, are targeted by the checkpoint to impose the cell cycle delay in response to defective recombination/synapsis; whether they are direct targets of Mek1 activity remains to be determined. The Swe1 kinase carries out the inhibitory phosphorylation of the main budding yeast cyclin-dependent kinase Cdc28 at Tyr19. In addition, inhibition and nuclear exclusion of the meiosis-specific transcription factor Ndt80 results in transcriptional down-regulation of a number of genes including those encoding B-type cyclins and the Cdc5 polo-like kinase that, together with inactive Cdc28, lead to meiotic cell cycle arrest (13–16).

Besides the Mec1-Ddc2/Tel1 sensors, the meiotic recombination checkpoint also shares other upstream components with the canonical DNA damage checkpoint, including Rad24 and the '9-1-1' (Rad17-Mec3-Ddc1) module, which interacts with Red1 (17). In addition, epigenetic regulators, such as the Sir2 histone deacetylase and the Dot1 histone methyltransferase, also operate in the meiotic checkpoint response, at least in part, by regulating the chromosomal distribution of the meiosis-specific Pch2 protein (8,18,19).

Pch2 (also known as TRIP13 in mammals) is an evolutionarily conserved AAA+ ATPase involved in various aspects of meiotic chromosome metabolism in an ample range of organisms, including budding yeast, plants, worms, flies and mice. Pch2 was initially discovered in *S. cerevisiae* as a component of the checkpoint responding to the meiotic defects of the synapsis-deficient *zip1* mutant lacking the central region of the SC (18,20). On the other hand, functional analyses of Pch2 in wild-type meiosis, has revealed that this ATPase negatively regulates the accumulation of the Hop1 protein at chromosome axes (18,21–23); in addition, functions for Pch2^{Trip13} in DSB generation, crossover interference, IH recombination bias, and regulation of rDNA recombination have been also described in both yeast and mouse (24–28). Intriguingly, whereas the absence of Pch2 bypasses the meiotic delay of the synapsis-deficient *zip1* mutant, it has little effect on the checkpoint response to unrepaired resected DSBs in *dmc1*. In contrast, Pch2 acting through Xrs2 and Tel1 (but not Mec1) signals unprocessed DSBs in *sae2* strains; however, Tel1 is not required for the *zip1*-induced synapsis checkpoint (29). All these pieces of evidence suggest that, depending on the initiating event, Pch2 may perform specific functions in relaying the checkpoint signal generated by different meiotic perturbations.

Whereas in budding yeast Pch2 appears to be dedicated exclusively to meiotic functions, the Trip13^{Pch2} homolog in metazoa is also involved in the mitotic spindle assembly checkpoint regulating the Mad2 protein, which, like Hop1, contains a HORMA domain (30–32). Underscoring the relevance of Trip13^{Pch2} function in somatic cells, the expression levels of Trip13^{Pch2} in certain types of cancer define the chemotherapy resistance and prognosis (33,34). Recent work has revealed the structural properties of this conserved ATPase and the conformational changes induced in some of its substrates (35).

In order to gain further insight into the functional impact of Pch2 during SC-deficient meiosis, we first describe here a genetic overexpression screen aimed to discover factors involved in the checkpoint role of Pch2. Despite the fact that Pch2 somehow promotes the turnover of Hop1 from meiotic chromosome axes; that is, Hop1 is more abundant and more continuous on *pch2* chromosomes, we surprisingly found that Hop1 overproduction suppresses the checkpoint defect of the *zip1 pch2* mutant. Then, we show that, in the *zip1* mutant, Pch2 is required for Mek1 autophosphorylation and formation of chromosomal Mek1 foci, and that *HOP1* overexpression restores full Mek1 activation in *zip1 pch2*. We also demonstrate that, in contrast with the *pch2* single mutant, Hop1 is not more abundant on *zip1 pch2* chromosomes; furthermore, in response to *zip1* defects, Pch2 specifically promotes high levels of Hop1 phosphorylation at Thr318 required to sustain checkpoint function. Finally, we show that *pch2* mutants carrying mutations in the Walker A or Walker B motifs phenocopy the defects of the *pch2* null-mutant, indicating that the ATPase activity of Pch2 is essential for its synapsis checkpoint function. Moreover, the Walker A-deficient Pch2 version fails to localize to the chromosomes and to form a stable complex suggesting that adenosine triphosphate (ATP) binding is required for formation or integrity of the Pch2 hexameric complex. We conclude that the critical function of the Pch2 ATPase in a *zip1*-deficient situation is to facilitate Mec1-dependent phosphorylation of Hop1 at Thr318.

MATERIALS AND METHODS

Yeast strains and meiotic time courses

The genotypes of yeast strains are listed in Supplementary Table S1. All strains are in the BR2495 or the BR1919 background (5,36). The *zip1::LEU2*, *zip1::LYS2*, *zip1::URA3*, *zip3::URA3*, *ecm11::kanMX6*, *ndt80::LEU2*, *ddc1::ADE2*, *rad17::LEU2*, *rad24::TRP1*, *dot1::TRP1*, *pch2::TRP1*, *sir2::LEU2*, *hop1::hphMX4* and *rad54::LEU2* gene deletions were previously described (5,8,15,18,19,37–39). The *rad51::natMX4* deletion was made following a PCR (polymerase chain reaction)-based approach (40). The *ndt80::kanMX3* construct was generated by marker swapping in *ndt80::LEU2* strains using the M3926 plasmid (41). The *pph3::kanMX6* cassette was amplified from genomic DNA of a W303-based strain containing that deletion (a gift from R. Bermejo; CIB-CSIC) and used to transform the appropriate BR1919 strains. For substitution of the *PCH2* gene for the *pch2Δ-lacZ::TRP1* construct, strains were transformed with the pSS67 plasmid (see below) digested with XhoI-SphI. N-terminal tagging of *PCH2* with

three copies of the HA epitope was previously described (18). *PCH2* was also tagged with three copies of the MYC epitope at the same position using identical procedures (42). The *MEK1-GFP* and *DDC2-GFP* constructs were also previously described (8,43). The *pch2-K320A* and *pch2-E399Q* mutations were introduced at the *PCH2* genomic locus using the *delitto perfetto* technique (44); they generate a NarI and a BstNI site, respectively, utilized for genotyping purposes during genetic crosses. The sequences of the primers used are available upon request. All strains were made by direct transformation or by genetic crosses always in an isogenic background. Sporulation conditions for meiotic time courses have been described (8). To score meiotic nuclear divisions, samples were taken at different time points, fixed in 70% Ethanol, washed in phosphate buffered saline (PBS) and stained with 1 μg/μl DAPI for 15 min. At least 300 cells were counted at each time point. Meiotic time courses were repeated several times; representative experiments are shown.

Plasmids

The plasmids used are listed in Supplementary Table S2. The pSS51 plasmid expressing a *pch2-lacZ* fusion was constructed by cloning a 1.3-kb XhoI-BamHI fragment containing the *PCH2* promoter and the N-terminal ORF region encoding the first 90 amino acids into the SalI-BamHI sites of the YCp50-derivative R1566 plasmid harboring the *E. coli lacZ* gene with a BamHI site at the 5′ end to generate an in-frame fusion. pSS67 contains a 4.3-kb BglII-NheI fragment from pSS51 harboring *pch2-lacZ* cloned into BglII-SphI of pSS53 (18). The R1692 plasmid overexpressing *HOP1* has been previously described (45). pSS54 contains a 3.2-kb KpnI-PstI *PCH2* fragment in the high-copy YEp352 vector. The pSS316 and pSS317 plasmids were constructed as follows: a 2.7-kb fragment containing *HOP1* ORF and the 5′ (648 bp) and 3′ (241 bp) UTR regions was first amplified by PCR from genomic DNA of a BR1919 strain using oligos HOP1-EcoRI(Fw) and HOP1-SalI(Rv) and blunt-cloned into the pJET1.2 vector (ThermoFisher Scientific) to originate pSS314. This *Eco*RI-*Sal*I fragment was then subcloned into pRS426 to generate the pSS316 plasmid. A 1.6-kb fragment spanning the *hop1-T318A* mutation was amplified from the JCY565 strain (6) (a gift from J. Carballo; CIB-CSIC), digested with BamHI-SacI and used to replace the same 1.0-kb fragment in pSS314 to generate pSS315. The 2.7-kb EcoRI-SalI fragment of pSS315 was then transferred to pRS426 to originate the pSS317 plasmid overexpressing *hop1-T318A*.

Genetic screen for high-copy suppressors of *zip1 pch2*

The *zip1 pch2-lacZ* mutant (DP221) was transformed with a yeast genomic library constructed in the multicopy vector YEp24 (46). Transformants were selected on SC-Ura and replica-plated to SPO plates containing a sterile Whatman 3MM filter paper on top. As positive controls, two colonies of DP221 transformed with pSS54 were placed at known positions on every plate. After incubation at 30°C for 3 days, the filters were removed, exposed to chloroform fumes for 10 min and assayed for β-galactosidase activity by incubating them at 30°C, colony side up, in empty dishes with a solution of 500 μl of Z-buffer (60 mM Na_2HPO_4, 40 mM NaH_2PO_4, 10 mM KCl, 1 mM $MgSO_4$, 40 mM β-mercatoethanol, pH 7.0) containing 100 μl of 20 mg/ml X-Gal. About 23 000 transformants were scored and 21 displayed blue color; plasmids were recovered for further analysis. The presence of *PCH2* in the plasmids was discarded by PCR using internal *PCH2* primers. Fifteen of the plasmids recovered fail to reproduce the phenotype when reintroduced into DP221, indicating that the suppression phenotype was not linked to the plasmids. The remaining six plasmids were analyzed by restriction mapping and sequencing of the insert ends and were grouped into two Pch-Two-Suppressors: *PTS10* containing *RPS9A* and a truncated form of *MOT1*, and *PTS11* containing *HOP1*, *PCI8*, *MAM33*, *RPS24B* and *SEC6*.

Western blotting and immunoprecipitation

Total cell extracts were prepared by trichloroacetic acid (TCA) precipitation from 5-ml aliquots of sporulation cultures as previously described (13). Analysis of Mek1 phosphorylation using Phos-tag gels was performed as reported (8). The antibodies used are listed in Supplementary Table S3. The ECL or ECL2 reagents (ThermoFisher Scientific) were used for detection. The signal was captured on films and/or with a ChemiDoc XRS system (Bio-Rad) and quantified with the Quantity One software (Bio-Rad).

For immunoprecipitation of Pch2, 5-ml aliquots from 16 h meiotic cultures were crosslinked with 1% formaldehyde for 10 min at 30°C. The reaction was quenched by adding glycine to 250 mM and incubating for 5 min on ice. Cells were collected, washed and broken with glass beads in lysis buffer (150 mM NaCl, 1% Triton X-100, 50 mM Tris HCl pH 8.0) containing protease inhibitors (Complete Ultra Tablets, Roche). Clarified extracts were immunoprecipitated with anti-HA antibodies conjugated with magnetic MicroBeads using the μMACS Epitope Tag Protein Isolation Kit (Miltenyi Biotec) following the manufacturer's protocol.

Cytology

Immunofluorescence of chromosome spreads and whole cells was performed essentially as described in (47) and (48), respectively. The antibodies used are listed in Supplementary Table S3. Images of spreads were captured with a Nikon Eclipse 90i fluorescence microscope controlled with MetaMorph software and equipped with a Hammamatsu Orca-AG CCD camera and a PlanApo VC 100 × 1.4 NA objective. Ddc2-GFP foci images were captured with an Olympus IX71 fluorescence microscope equipped with a personal DeltaVision system, a CoolSnap HQ2 (Photometrics) camera and 100x UPLSAPO 1.4 NA objective. Stacks of 10 planes at 0.4 μm intervals with 500 ms exposure time were captured. Maximum intensity projections of deconvolved images were generated using the SoftWorRx 5.0 software (Applied Precisions). Quantification of the fluorescence signal in individual spread nuclei or cells was performed with the Image J software. Background signal was subtracted using the Otsu's threshold method of Image J.

DAPI images were collected using a Leica DMRXA fluorescence microscope equipped with a Hammamatsu Orca-AG CCD camera and a 63 × 1.4 NA objective.

Dityrosine fluorescence assay, sporulation efficiency and spore viability

To examine dityrosine fluorescence as an indicator of the formation of mature asci, patches of cells grown on YPDA plates were replica-plated to sporulation plates overlaid with a nitrocellulose filter (Protran BA85, Whatman). After 3-days incubation at 30°C, fluorescence was visualized by illuminating the open plates from the top with a hand-held 302 nm UV lamp. Images were taken using a Gel Doc XR system (Bio-Rad). Sporulation efficiency was quantitated by microscopic examination of asci formation after 3 days on sporulation plates. Both mature and immature asci were scored. At least 300 cells were counted for every strain. Spore viability was assessed by tetrad dissection. At least 144 spores were scored for every strain.

Statistics

To determine the statistical significance of differences a two-tailed Student *t*-test was used. *P*-Values were calculated with the GraphPad Prism 5.0 software.

RESULTS

A genetic screen for high-copy suppressors of *zip1 pch2* identifies *HOP1*

The absence of Pch2 alleviates the checkpoint-induced meiotic arrest of the *zip1* mutant. To gain insight into the function of Pch2 in this checkpoint we devised a genetic screen to identify genes that, when overexpressed, restored the meiotic block in a *zip1 pch2* double mutant. This screen could potentially identify novel components of the checkpoint pathway and/or reveal additional functional interactions of Pch2 with previously known checkpoint factors. We took advantage of the fact that Pch2 is transiently produced during meiotic prophase in the wild type, but it accumulates in the prophase-arrested *zip1* mutant (18). To follow *PCH2* expression, we generated a construct containing the *PCH2* coding sequence corresponding to the first 90 amino acids (*pch2Δ*$^{90\text{-}564}$) fused the *E. coli lacZ* gene and expressed from the *PCH2* promoter in a centromeric plasmid (Figure 1A). β-galactosidase activity was used as a readout for *PCH2* expression and dityrosine fluorescence as an indicator of sporulation on plates. Consistent with the previously described *PCH2* expression pattern, meiotic-proficient wild-type cells containing this plasmid exhibited no or low levels of β-galactosidase activity, but the prophase-arrested *zip1* mutant accumulated high levels of β-galactosidase activity, manifested as blue color on sporulation plate assays (Figure 1B and C). Alleviation of the prophase arrest in a *zip1 dot1* mutant (8,19) eliminated β-galactosidase production (Figure 1B), whereas the checkpoint-independent meiotic block imposed by deletion of *NDT80* (49) resulted in β-galactosidase accumulation (Figure 1B). Thus, the *pch2Δ*$^{90\text{-}564}$*-lacZ* fusion gene (hereafter, *pch2Δ-lacZ*) serves as a useful reporter for meiotic prophase arrest.

We next generated diploid strains in which both copies of the *PCH2* gene were replaced by the *pch2Δ-lacZ* construct at the genomic locus (Figure 1D). As expected, *pch2Δ-lacZ* behaved like a null mutant; it bypassed checkpoint arrest as manifested by the presence of dityrosine fluorescence in *zip1 pch2Δ-lacZ*, but no β-galactosidase was detected (Figure 1E). Notably, introduction of a single-copy or a high-copy *PCH2* restored the meiotic block in *zip1 pch2Δ-lacZ* and resulted in conspicuous β-galactosidase accumulation (Figure 1E). Thus, we reasoned that we could use this assay to screen for high-copy suppressors of the unscheduled sporulation resulting from the defective checkpoint in *zip1 pch2Δ-lacZ*. After transformation with a 2μ-based high-copy genomic library and replica-plate to sporulation medium, we scored for the appearance of blue color as an indicator of restored meiotic prophase arrest (Figure 1F and G). The plasmids contained in the colonies displaying β-galactosidase activity were recovered, analyzed by restriction digestion and DNA sequencing, and re-transformed into the original *zip1 pch2Δ-lacZ* strain to confirm that the suppression phenotype was linked to the plasmid. In addition to clones containing *PCH2*, we isolated two different high-copy suppressor genes (*PTS*, for Pch Two-Suppressors). *PTS10* encoded a C-terminal truncated version of the Mot1 transcriptional regulator (50). Since *2μPTS10* only conferred a transient and partial restoration of the meiotic arrest (Figure 1H) it was not further analyzed. In contrast, the effect of *2μPTS11* was comparable to that of the *2μPCH2* control (Figure 1H). Sequencing analysis revealed that the *HOP1* gene was present in the *2μPTS11* plasmids isolated from the library. To confirm that high levels of Hop1 were indeed responsible for the phenotype we analyzed a previously characterized *2μHOP1* plasmid (8,45) and found a similar effect on suppression of *zip1 pch2Δ-lacZ* sporulation (Figure 1H). Thus, *HOP1* overexpression restores meiotic arrest in the checkpoint-deficient *zip1 pch2Δ-lacZ* mutant.

Overexpression of *HOP1* suppresses the checkpoint defect of *pch2*, *sir2* and *dot1*, but not that of *rad17*, *ddc1* and *rad24* mutants

To determine whether the effect of Hop1 overproduction was exclusively exerted when the checkpoint was inactivated by the absence of Pch2, we analyzed mutants in other checkpoint genes also required for the *zip1* meiotic block. The Rad17, Ddc1 and Rad24 proteins are members of the 9-1-1 and RFC complexes acting upstream in the checkpoint pathway and contributing to the activation of the Mec1-Ddc2 sensor kinase (6,51,52). On the other hand, the H3K79 methyltransferase Dot1 is required for proper phosphorylation and localization of the Hop1 adaptor and the Mek1 checkpoint effector kinase (8). Dot1 regulates the chromosomal distribution of the nucleolar-associated Pch2 and Sir2 proteins (8,19). As shown in Figure 2, Hop1 overproduction significantly reduced sporulation efficiency in *zip1 pch2*, *zip1 sir2* and *zip1 dot1*, but had no effect on *zip1 rad17*, *zip1 ddc1* and *zip1 rad24* mutants. Thus, *HOP1* overexpression specifically supports meiotic checkpoint function when the Dot1-Pch2 module is not operative.

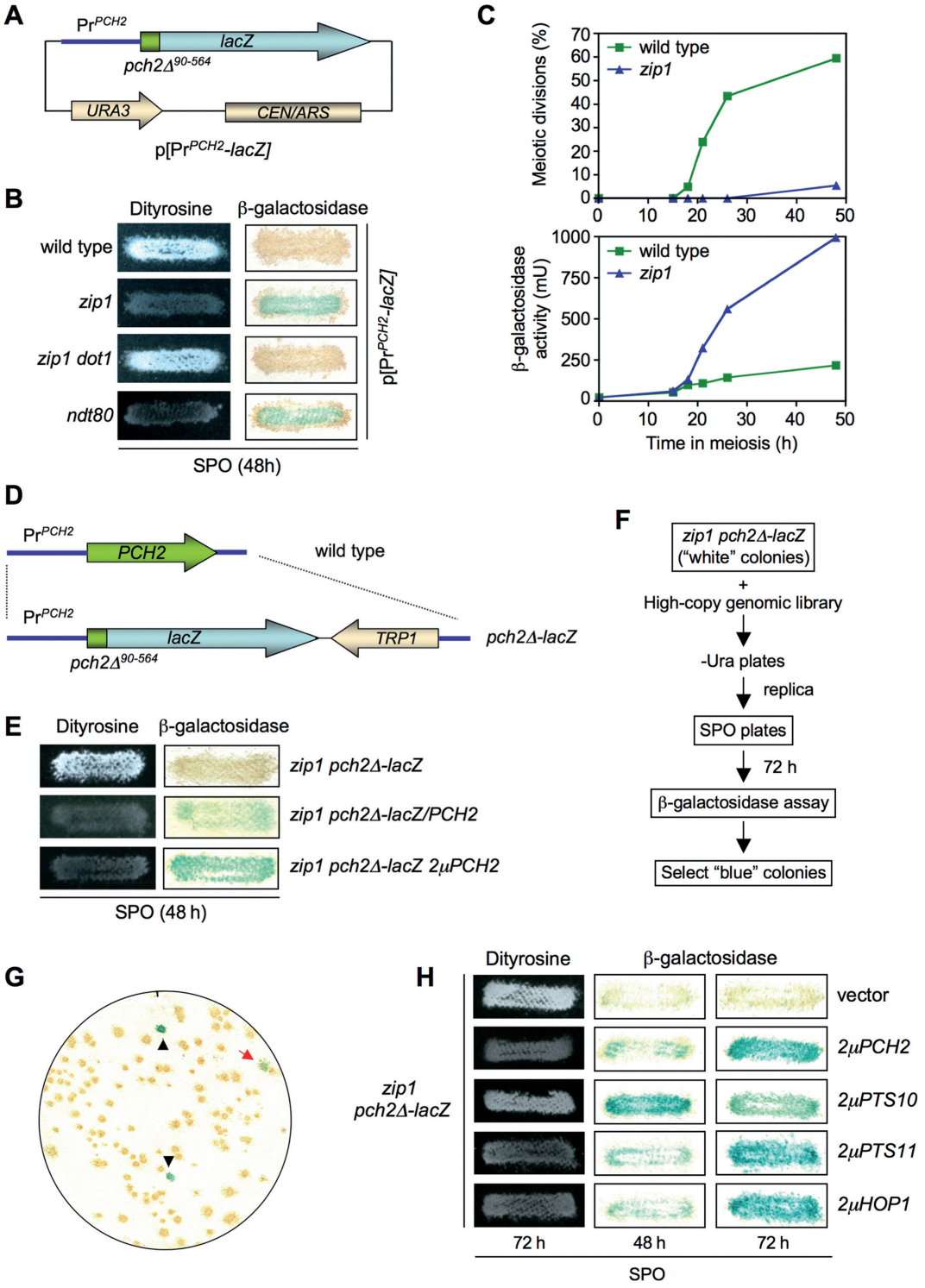

Figure 1. Identification of *HOP1* in a genetic screen for high-copy suppressors of the *zip1 pch2* checkpoint defect using a *pch2-lacZ* construct as a reporter for meiotic prophase arrest. (**A**) Schematic representation of a centromeric plasmid (pSS51) carrying the *PCH2* promoter and the coding sequence for the first N-terminal 90 amino acids fused in frame with the bacterial *lacZ* gene. (**B**) Dityrosine fluorescence and β-galactosidase assays of the indicated strains transformed with the pSS51 plasmid after 48 h on sporulation plates. (**C**) Kinetics of meiotic divisions and β-galactosidase activity in meiotic time courses of wild-type and *zip1* strains containing the pSS51 plasmid. (**D**) Schematic representation of the substitution of the *PCH2* gene for the *pch2-lacZ* construct at the genomic locus. (**E**) Dityrosine fluorescence and β-galactosidase assays of the indicated strains after 48 h on sporulation plates. (**F**) Scheme of the genetic screen. (**G**) Representative β-galactosidase assay of a plate from *zip1 pch2Δ-lacZ* transformed with the genomic high-copy library. Black triangles indicate positive controls deliberately placed at known positions on every plate of the screen. The red arrow points to a positive 'blue' candidate. (**H**) Dityrosine fluorescence and β-galactosidase assays of the *zip1 pch2Δ-lacZ* strain transformed with the indicated plasmids. Strains for (B) and (C) are: BR2495 (wild type), MY63 (*zip1*), DP174 (*zip1 dot1*) and S3483 (*ndt80*). Strains for (E), (F), (G) and (H) are: DP221 (*zip1 pch2Δ-lacZ*) and DP228 (*zip1 pch2Δ-lacZ/PCH2*). DP221 was transformed with empty vector or the indicated high-copy plasmids.

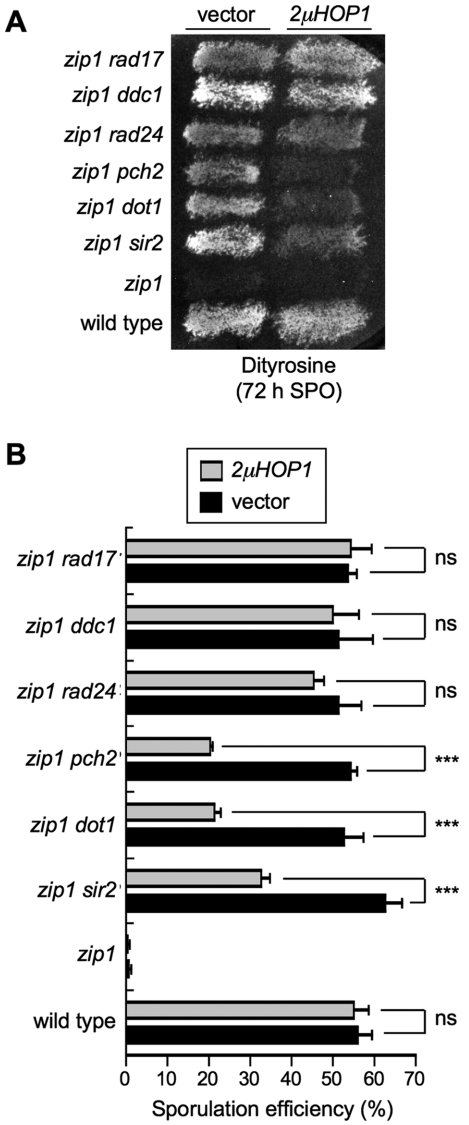

Figure 2. High-copy *HOP1* specifically suppresses the checkpoint defect of *zip1 pch2*, *zip1 sir2* and *zip1 dot1*. (**A**) Dityrosine fluorescence assay of the indicated strains transformed with empty vector (YEp352) of high-copy *HOP1* (R1692) after 3 days on sporulation plates. (**B**) Microscopic quantification of the sporulation efficiency of the strains analyzed in (A). Three independent counts were performed. Means and standard deviations are shown. (ns), no significant difference; (***), $P < 0.001$. Strains are: BR2495 (wild type), MY63 (*zip1*), DP174 (*zip1 dot1*), DP223 (*zip1 pch2*), DP267 (*zip1 sir2*), S4295 (*zip1 rad24*), S4278 (*zip1 ddc1*) and S4286 (*zip1 rad17*).

HOP1 overexpression restores meiotic checkpoint activity in *zip1 pch2*

To further explore the effect of *HOP1* overexpression, we next analyzed meiotic kinetics and molecular markers of checkpoint activation, such as Mek1 phosphorylation (in phostag gels) and Cdc5 inhibition, during meiotic time courses of wild-type, *zip1* and *zip1 pch2* strains with or without Hop1 overproduction (Figure 3). In the wild type, the Mek1 kinase was only weakly and transiently activated (Figure 3A) (8); *HOP1* overexpression slightly prolonged Mek1 activation resulting in a subtle meiotic delay (Figure 3A and B). As expected, the synapsis-deficient *zip1* mutant showed extensive Mek1 phosphorylation, delayed Cdc5 production and a significant meiotic delay; Hop1 overproduction slightly enhanced those effects (Figure 3C and D). Consistent with the defective checkpoint, Mek1 hyperactivation was not observed in the *zip1 pch2* mutant; moreover, Cdc5 production and meiotic divisions displayed roughly wild-type kinetics (Figure 3E and F). However, high doses of Hop1 markedly restored Mek1 phosphorylation, delayed Cdc5 production and provoked a significant meiotic delay in *zip1 pch2* (Figure 3E and F).

To elude the possible effect of the different kinetics of meiotic progression in the strains analyzed in these assays, we assessed Mek1 activation and localization in pachytene-arrested *ndt80* cells. To achieve full activation, Mek1 undergoes Mec1/Tel1-dependent phosphorylation followed by *in trans* autophosphorylation (6,9). The different forms resulting from these two phosphorylation events can be resolved in phostag gels (8) (Figure 3G, black and white arrows). We found that Mec1/Tel1-dependent phosphorylation occurred in the absence of Pch2 (Figure 3G, black arrow). However, the bands corresponding to Mek1 autophosphorylation were absent in *zip1 pch2* transformed with empty vector (Figure 3G, white arrows) indicating that, like Dot1, Pch2 is specifically required for Mek1 autophosphorylation. Strikingly, complete Mek1 activation was reestablished in *zip1 pch2* cells overproducing Hop1 (Figure 3G).

The *zip1*-induced meiotic checkpoint also promotes the formation of chromosome-associated Mek1 foci (8,53) (Figure 3H). Like Mek1 phosphorylation, formation of Mek1 foci was also impaired in *zip1 pch2*, which displayed fewer and dimmer foci. In contrast, numerous bright Mek1 foci were observed in the *zip1 pch2* mutant overexpressing *HOP1* (Figure 3H).

Taken together, these results indicate that Pch2 is required for Mek1 autophosphorylation and localization when the synapsis checkpoint is activated by the lack of Zip1. In the absence of Pch2, artificially-induced high levels of Hop1 can support checkpoint activity suggesting that Hop1 function is somehow compromised in the *zip1 pch2* mutant resulting in impaired Mek1 activation.

Pch2 is required for Hop1 phosphorylation induced by the synapsis checkpoint

Several lines of evidence indicate that, in unperturbed meiosis, Pch2 promotes the turnover of Hop1 from chromosomes; the *pch2* single mutant displays a more abundant and continuous localization of Hop1 along synapsed chromosomes (18,22). Thus, in principle, it was rather surprising that high doses of Hop1 could compensate for the absence of Pch2 supporting Mek1 activation and checkpoint function in the *zip1 pch2* mutant. To investigate this apparent contradiction, we examined Hop1 production, localization and phosphorylation in wild type, *pch2*, *zip1* and *zip1 pch2* prophase-arrested *ndt80* cells. Pachytene checkpoint activation leads to Mec1/Tel1-dependent phosphorylation of Hop1 at defined S/T-Q sites; in particular, phosphorylation of the T318 residue is critical for Hop1 checkpoint function promoting Mek1 activation (6,7). As expected, both on chromosome spreads and in whole-cell lysates, we found

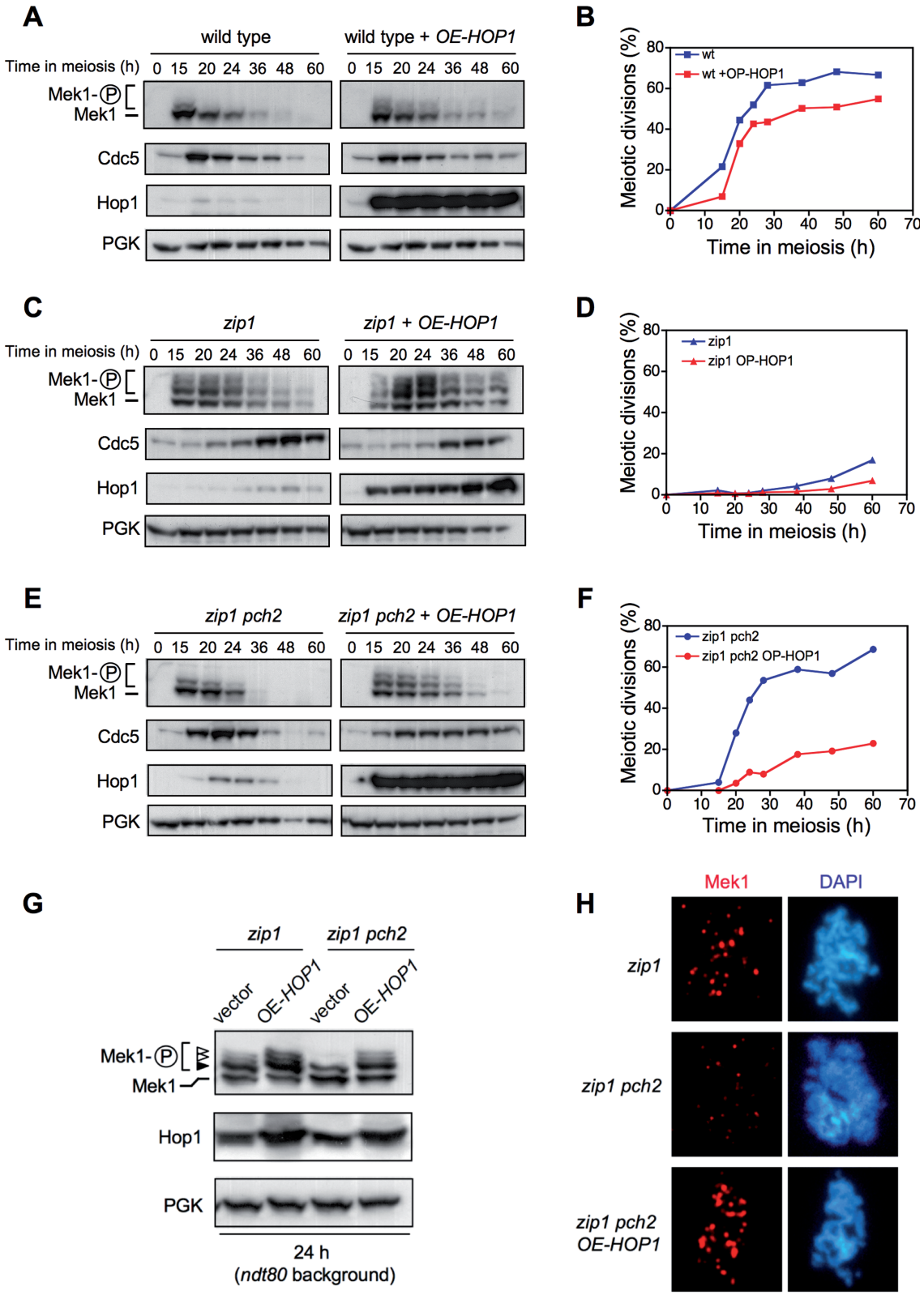

Figure 3. *HOP1* overexpression largely restores meiotic arrest, Mek1 activation, Mek1 localization and delayed Cdc5 production in *zip1 pch2*. Western blot analysis of the indicated proteins and meiotic kinetics of (**A** and **B**) wild type, (**C** and **D**) *zip1* and (**E** and **F**) *zip1 pch2* transformed with empty vector (pRS426) or high-copy *HOP1* (R1692). Strains are: DP421 (wild type), DP422 (*zip1*) and DP1029 (*zip1 pch2*). (**G**) Analysis of Mek1 phosphorylated forms in *ndt80*-arrested strains. The black arrowhead marks the Mec1/Tel1-dependent band and the white arrowheads point to the forms resulting from Mek1 autophosphorylation (8). Strains are: DP428 (*zip1*) and DP881 (*zip1 pch2*), transformed with pRS426 (empty vector) or R1692 (OE-*HOP1*). (**H**) Analysis of Mek1 localization by immunofluorescence of spread meiotic chromosomes using anti-GFP antibodies. Representative nuclei are shown. Strains are DP582 (*zip1*) and DP1111 (*zip1 pch2*).

higher levels of Hop1 in the *pch2* single mutant, compared with the wild type (Figure 4Aa,b; B and D). Paralleling the accumulation of total Hop1, an increased number of phospho-Hop1^{T318} foci (Figure 4Ae,f; C) and higher levels of the phosphorylated protein (Figure 4D) were also observed in *pch2*. Nevertheless, the ratio of phospho-Hop1^{T318} relative to total Hop1 was only moderately increased in *pch2* compared with the wild type (Figure 4E). In fact, the Mek1 kinase is minimally activated in *pch2* as manifested by the almost complete absence of autophosphorylation (Figure 4D, white arrow), the low level of histone H3T11 phosphorylation, which is a target of Mek1 (54) and, therefore, a useful reporter of its kinase activity (Figure 4D), and the rather normal kinetics of meiotic progression of *pch2*, which only shows a minor delay (20) (see also Figure 8D below).

On the other hand, the *zip1* mutant displayed continuous Hop1 signal along unsynapsed chromosome axes (55) (Figure 4Ac and B), numerous and strong phospho-Hop1^{T318} foci (Figure 4Ag and C), and high levels of phospho-Hop1^{T318} protein (Figure 4D). Importantly, the phospho-Hop1^{T318}/total Hop1 ratio was significantly raised in *zip1* (Figure 4E), leading to full activation of Mek1 and robust H3T11 phosphorylation (Figure 4D). Deletion of *PCH2* in *zip1* resulted in increased global levels of the Hop1 protein detected by Western blot, as compared with the *zip1* single mutant (Figure 4D); however, it was not massively incorporated on the axes; Hop1 chromosomal distribution in the *zip1 pch2* double mutant was less continuous than in *zip1* (Figure 4Ad and B). Importantly, *zip1*-induced Hop1^{T318} phosphorylation was dramatically reduced in the absence of Pch2 (Figure 4Ah, C, D and E), thus explaining the impaired Mek1 activation and defective checkpoint response in *zip1 pch2* (Figures 3 and 4D).

These observations reveal that the critical role of Pch2 in the *zip1*-induced checkpoint is to promote Hop1 phosphorylation at T318. Confirming this notion, overexpression of wild-type *HOP1*, but not that of a phosphorylation-deficient *hop1-T318A* mutant (6), restored Hop1^{T318} phosphorylation and checkpoint function (i.e. full Mek1 activation) in *zip1 pch2* (Figure 5).

The absence of PP4 restores checkpoint activity in *zip1 pch2* to a small extent

It has been reported that the protein phosphatase 4 (PP4) counteracts Mec1/Tel1-dependent Hop1^{T318} phosphorylation (7); therefore, to further explore the role of Pch2 in controlling Hop1^{T318} phosphorylation we examined the effect of deleting the *PPH3* gene, which encodes the catalytic subunit of PP4. We analyzed the kinetics of meiotic divisions (Figure 6A) and the activation of molecular markers of the checkpoint, including Hop1^{T318}, Mek1 and histone H3T11 phosphorylation (Figure 6B). Consistent with a role for PP4 in shutting off pachytene checkpoint signaling, the *pph3* mutant showed a transient Hop1-Mek1 activation (Figure 6B) manifested as a short meiotic delay (Figure 6A); moreover, the *zip1 pph3* double mutant displayed persistent checkpoint activity and strong meiotic arrest (Figure 6A and B). Although Hop1^{T318} phosphorylation is severely impaired in *zip1 pch2* (Figures 4D, E and 6B), the lack of PP4 resulted in higher levels of Hop1^{T318} phosphorylation and the ensuing Mek1 kinase activity (Figure 6B) leading to delayed meiotic divisions in *zip1 pch2 pph3* compared to *zip1 pch2* (Figure 6A). However, checkpoint function (i.e. Hop1^{T318} phosphorylation) was not completely restored in the *zip1 pch2 pph3* triple mutant, which showed faster meiotic progression than that of *zip1* and a weaker and shorter Mek1 activation (Figure 6A and B).

All together, these observations confirm that Pch2 specifically supports Hop1^{T318} phosphorylation when the synapsis checkpoint is triggered by the absence of Zip1 and reveal that the control of Hop1^{T318} phosphorylation by Pch2 is not, at least exclusively, exerted by modulating PP4 action.

To determine whether the defective Hop1^{T318} phosphorylation in *zip1 pch2* stems from an impaired general activation of the Mec1-Ddc2 complex, we performed immunofluorescence of spread meiotic chromosome using an antibody that recognizes the phosphorylated S/T-Q motifs. As shown in Supplementary Figure S1A, phospho-S/T-Q foci similarly decorated both *zip1* and *zip1 pch2* chromosomes. We also examined the localization of the Mec1-Ddc2 complex monitoring the induction of Ddc2-GFP foci when the meiotic checkpoint is triggered in *zip1* cells (43). We found that the formation of Ddc2 foci is not altered by the absence of Pch2 in *ndt80*-arrested cells (Supplementary Figure S1B). These observations suggest that Pch2 does not impact widespread Mec1 signaling.

Unsynapsed chromosomes and unrepaired DSBs remain in *zip1 pch2 ndt80*

Although the precise defect(s) triggering the checkpoint in *zip1* mutants (defective synapsis and/or unrepaired DSBs) remains unclear, since *pch2* affects meiotic DSB metabolism, it was formally possible that the reduced Hop1^{T318} phosphorylation observed in *zip1 pch2* resulted from the absence or the disappearance of the checkpoint-activating signal. However, the fact that Ddc2 foci formation and S/T-Q phosphorylation are conspicuous in *zip1 pch2* (Supplementary Figure S1) indicates that the *zip1* defects triggering the checkpoint are still present in the absence of Pch2. We also monitored the presence of Rad51 foci as a marker for unrepaired DSBs (56). To avoid again the effect of meiotic progression on DSB repair outcome we performed the analysis in *ndt80* cells. No or few Rad51 foci were observed in most wild-type (1.8 $\pm$ 0.3 SEM foci per nucleus; n = 40) and *pch2* (2.0 $\pm$ 0.5 SEM foci per nucleus; n = 35) nuclei, but the number was markedly increased in the *zip1* mutant (5.5 $\pm$ 0.5 SEM foci per nucleus; n = 35). Importantly, although the fraction of unrepaired DSBs was reduced in *zip1 pch2* (3.5 $\pm$ 0.5 SEM foci per nucleus; n = 45), likely due to intersister (IS) repair, the double mutant still showed prominent Rad51 foci (Figure 7A). In addition, chromosome axes are unsynapsed in *zip1 pch2*; i.e., the synapsis defect continues to exist (Figure 4Ac,d). Thus, these observations indicate that the inability of *zip1 pch2* to phosphorylate Hop1 at T318 does not stem from the absence of defects triggering the checkpoint and point to a more direct role for Pch2 in controlling Hop1-Mek1 activation.

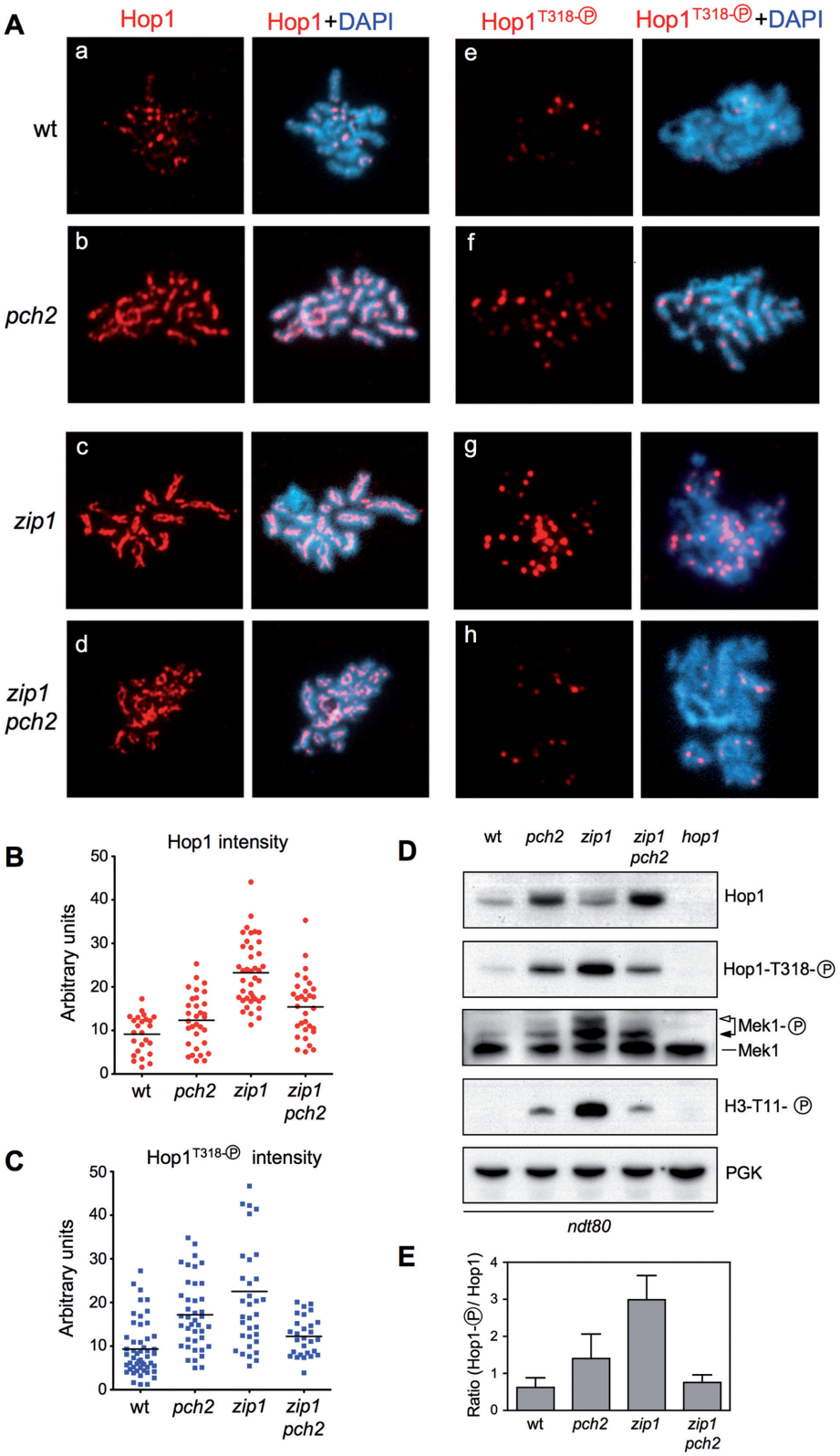

Figure 4. Pch2 promotes Hop1^{T318} phosphorylation in *zip1*. (**A**) Immunofluorescence of spread meiotic chromosomes stained with DAPI (blue) and anti-Hop1 (a-d panels) or anti-phospho-Hop1^{T318} (e–h panels) antibodies (red). Representative nuclei are shown. (**B** and **C**) Quantification of total Hop1 and phospho-Hop1^{T318} fluorescence signal, respectively, on the spreads analyzed in (A). Each spot in the plot represents the intensity of a nucleus scored. (**D**) Western blot analysis of the indicated proteins and phosphorylation events. (**E**) Quantification of relative Hop1^{T318} phosphorylation analyzed as in (D). The ratio of phospho-Hop1^{T318} versus total Hop1 chemiluminiscence signal is represented. Means and standard deviations from three independent experiments are shown. Strains are: DP424 (wild type), DP1058 (*pch2*), DP428 (*zip1*), DP881 (*zip1 pch2*) and DP700 (*hop1*). Spreads and lysates were prepared 24 h after meiotic induction of *ndt80* cells. For DP700 the sample was taken at 17 h.

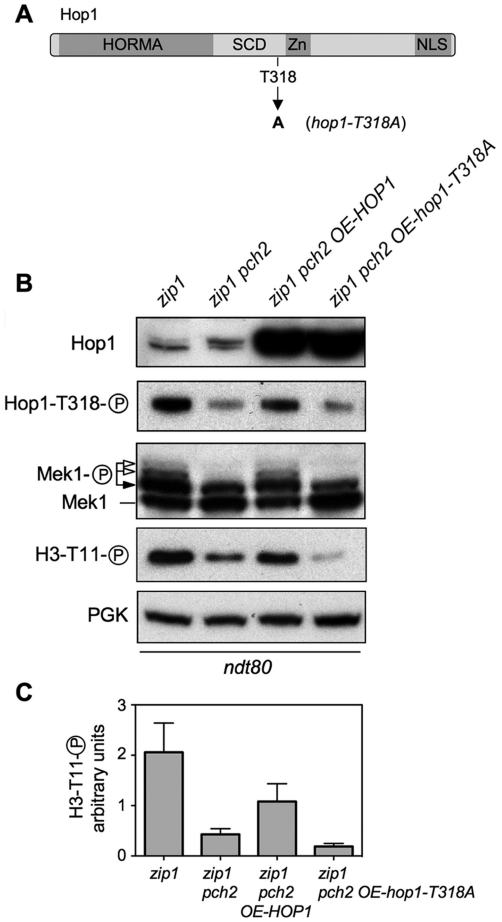

Figure 5. Hop1^{T318} phosphorylation is the critical checkpoint event impaired in *zip1 pch2*. (**A**) Schematic representation of the Hop1 protein domains and the position of the mutated T318 phosphosite (6) (**B**) Overexpression of wild-type *HOP1*, but not the *hop1-T318A* mutant, restores Mek1 activation in *zip1 pch2*. Western blot analysis of Hop1, phospho-Hop1^{T318}, Mek1 and phospho-H3^{T11} in *ndt80*-arrested cells. (**C**) Quantification of the phospho-H3^{T11} signal from three experiments. Note that Mek1 activity markedly increases, but is not fully restored in *zip1 pch2 OE-HOP1* cells due to plasmid-loss events in the meiotic cultures (43); those cells that lose the plasmid do not overproduce Hop1 and do not contribute to Mek1 phosphorylation. Strains are DP428 (*zip1*) and DP881 (*zip1 pch2*) transformed with pRS426 (empty vector), pSS316 (*OE-HOP1*) or pSS317 (*OE-hop1-T318A*).

The Pch2-Hop1-Mek1 signaling module impacts meiotic cell cycle progression

Since the analyses described above were performed in *ndt80*-arrested cells, we also explored the possibility that the mutation of *PCH2* suppresses *zip1* meiotic arrest exclusively by allowing the repair of DSBs by recombination between sister chromatids as a result of the impaired Mek1 function in *zip1 pch2* (28). If that were the case; that is, Mek1 only controls recombination partner choice and not cell cycle events, compromising repair by mutation of recombination factors would restore meiotic cell cycle arrest in *zip1 pch2* cells; therefore, we deleted *RAD51* to interfere with DNA repair. In parallel with monitoring meiotic divisions, we used the presence of multiple Ddc2-GFP foci as a reporter for unrepaired Spo11-dependent meiotic recombination intermedi-

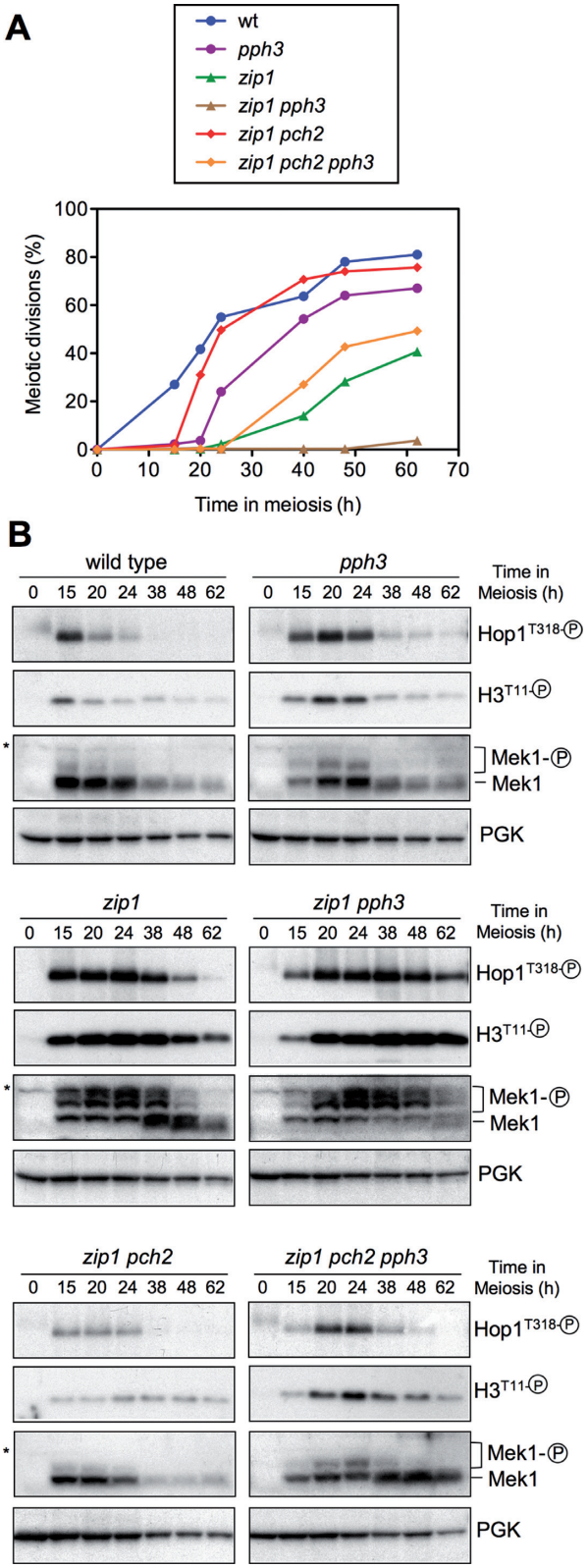

Figure 6. Impact of the PP4 phosphatase on Pch2-dependent meiotic checkpoint. (**A**) Time course of meiotic nuclear divisions; the percentage of cells containing two or more nuclei is represented. (**B**) Western blot analysis of Hop1^{T318} phosphorylation and Mek1 activity at the indicated time points in meiosis. PGK was used as a loading control. Strains are: DP421 (wild type), DP1247 (*pph3*), DP422 (*zip1*), DP1249 (*zip1 pph3*), DP1029 (*zip1 pch2*) and DP1245 (*zip1 pch2 pph3*).

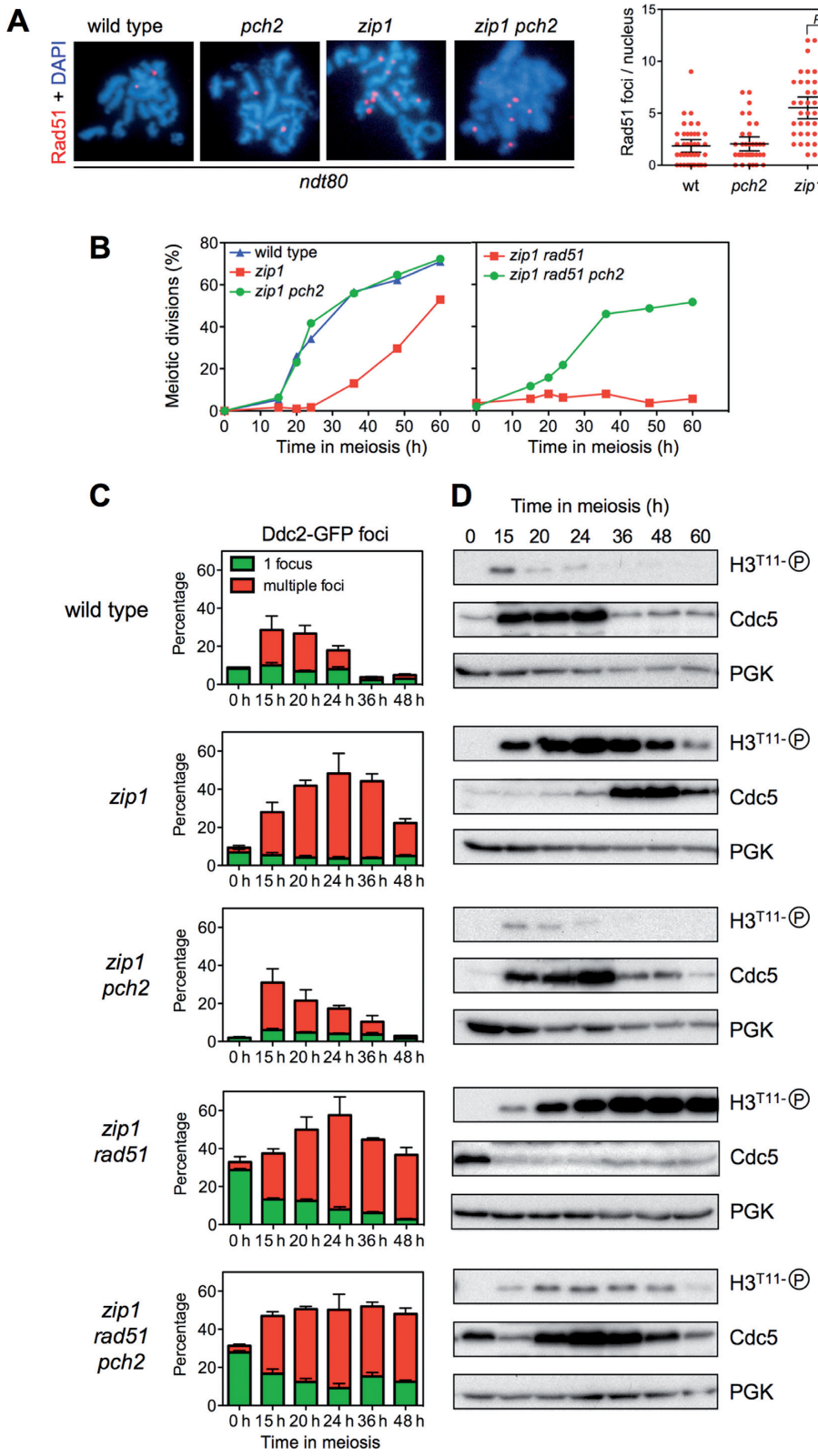

Figure 7. Effect of Pch2 on cell cycle progression and resolution of *zip1*-induced recombination intermediates. (**A**) Localization and quantification of Rad51 foci as markers for unrepaired DSBs on spread meiotic nuclei of *ndt80* cells after 24 h of meiotic induction. Strains are: DP424 (wild type), DP1058 (*pch2*), DP428 (*zip1*) and DP881 (*zip1 pch2*). (**B**) Time course of meiotic nuclear divisions. The percentage of cells with two or more nuclear masses is represented. (**C**) Quantification of Ddc2-GFP foci throughout meiosis. The percentage of cells containing a single non-meiotic Ddc2 focus (green bars) or multiple meiotic Ddc2 foci (red bars) from three different counts is represented. Note that *rad51* cells accumulate spontaneous non-meiotic Ddc2 foci at time zero. Between 150 and 800 cells were scored for each strain at every time point. (**D**) Western blot analysis of phospho-H3T11 (as a reporter for Mek1 activity), Cdc5 (as a marker for meiosis I entry) and PGK (as a loading control) from the same cultures analyzed in (B) and (C). Strains for (B), (C) and (D) are: DP448 (wild type), DP449 (*zip1*), DP1379 (*zip1 pch2*) DP1381 (*zip1 rad51*) and DP1382 (*zip1 pch2 rad51*).

ates (43), H3T11 phosphorylation as a reporter for Mek1 activity and Cdc5 production as a molecular indicator of prophase I exit and entry into meiotic divisions (Figure 7B, C and D). In the wild type, only a transient peak of Ddc2-containing cells was detected because recombination is normally completed. In the *zip1* mutant, cells containing multiple Ddc2 foci accumulate, leading to Mek1 activation and delayed Cdc5 production. As expected, the *zip1 pch2* double mutant showed impaired Mek1 activation allowing normal meiotic progression and the disappearance of recombination intermediates (Figure 7B, C and D). Notably, whereas at late time points a fraction of *zip1* cells underwent meiotic divisions after a delay, the *zip1 rad51* double mutant displayed a much tighter arrest (Figure 7B) and markedly reduced and delayed Cdc5 production (Figure 7D). Likewise, Ddc2 multiple foci and Mek1 activation persisted for longer in *zip1 rad51* (Figure 7C and D; Supplementary Figure S2). These observations indicate that compromising recombination by the *rad51* mutation prevents the resolution of recombination intermediates in *zip1* leading to a stronger meiotic block. Importantly, deletion of *PCH2* reduced Mek1 activation and restored meiotic progression and earlier Cdc5 production in *zip1 rad51* despite the persistence of multiple Ddc2 foci; that is, unrepaired recombination intermediates (Figure 7B,C,D; Supplementary Figure S2).

We also analyzed the effect of Rad54, which is a Rad51 accessory factor, and a direct Mek1 target (12). In addition to the action of Hed1, phosphorylation of Rad54 by Mek1 reduces its affinity for Rad51 binding; therefore, mutation of *RAD54* can be used also as a tool to interfere with meiotic recombinational repair (57–59). We observed that, like in *zip1 pch2*, the sporulation block of *zip1* was still relieved in the *zip1 pch2 rad54* triple mutant (Supplementary Figure S3A). Consistent with impaired repair in the absence of Rad54, spore viability was further reduced in *zip1 pch2 rad54* (29.1%, n = 144) compared with *zip1 pch2* (47.2%; n = 144). Moreover, we used chromosome spreads to monitor the presence of Ddc2 foci in combination with spindle staining as a sensitive cytological assay for checkpoint function (19,43,51). Whereas *zip1 rad54* cells arrested in prophase with unseparated SPBs and numerous Ddc2 foci (35.4 ± 2.5 SEM foci per nucleus; n = 13), *zip1 rad54 pch2* nuclei displaying elongated meiosis I spindle coexisting with persistent recombination intermediates (14.0 ± 3.0 SEM Ddc2 foci per nucleus; n = 10) could be detected (Supplementary Figure S3B). In wild-type nuclei, recombination intermediates never coexist with metaphase spindles (19,43,51). These findings indicate that, in the absence of Pch2, a late cell cycle event has been initiated before an earlier one has been completed; that is, checkpoint function is impaired.

In summary, these observations argue that Pch2 controls a general checkpoint response via Hop1-Mek1 regulation that includes the cell-cycle arrest outcome and not only the regulation of recombination.

To determine whether the effect of Pch2 was exerted exclusively in response to the meiotic defects resulting from the lack of Zip1, we examined other mutants affecting SC dynamics, such as *zip3* and *ecm11*. Zip3 is a SUMO ligase constituting the so-called synapsis initiating complex (60,61) and Ecm11 is a component of the central element of the SC (39,62). Similar to *zip1*, although to different extents, both *ecm11* and *zip3* single mutants displayed delayed meiotic progression (Supplementary Figure S4A), increased Hop1-T318 phosphorylation and induced Mek1 activity (Supplementary Figure S4B). Deletion of *PCH2* resulted in faster meiotic progression and impaired Hop1 and Mek1 activation (Supplementary Figure S4). Therefore, Pch2 impact on Hop1-Mek1 signaling is also required to restrain meiotic divisions in other mutants altering SC proper development.

The ATPase activity of Pch2 is required for its checkpoint function

Pch2 is a hexameric ring AAA+ ATPase (63). In order to investigate whether Pch2 ATPase activity is required for its meiotic checkpoint function, conserved critical residues in the AAA+ domain of Pch2 were mutated to abolish its catalytic activity (64). In particular, the lysine 320 in the Walker A motif required for ATP binding was changed to alanine, and the glutamic acid at position 399 in the Walker B motif, required for ATP hydrolysis, was substituted for glutamine to generate the *pch2-K320A* and *pch2-E399Q* mutants, respectively (Figure 8A). We used the *delitto perfetto* technique, which leaves no additional modifications, to introduce these mutations in the genomic loci of strains carrying functional N-terminal HA- or MYC-tagged versions of *PCH2* (18). Both Pch2-K320A and Pch2-E399Q mutant proteins were produced at normal levels and with normal kinetics (Figure 8B). Like *pch2Δ*, the *pch2-K320A* and *pch2-E399Q* single mutants showed no prominent phenotype in unperturbed meiosis; they were able to complete meiosis and sporulation with kinetics and efficiency similar to the wild type, producing high levels of viable spores (Figure 8C and D; Table 1). Interestingly, when the meiotic checkpoint was triggered by the lack of Zip1, we found that, like *pch2Δ*, the *pch2-K320A* and *pch2-E399Q* mutations completely suppressed the sporulation defect of *zip1* (Figure 8C); the *zip1 pch2-K320A* and *zip1 pch2-E399Q* double mutants displayed fairly normal kinetics of meiotic divisions (Figure 8D), but generate largely inviable meiotic products (Table 1). These observations imply that the ATPase activity of Pch2 is absolutely required to restrain meiotic progression when the checkpoint is induced by the absence of Zip1. To further confirm this interpretation we assessed the effect of the *pch2-K320A* and *pch2-E399Q* mutations on checkpoint function by monitoring molecular markers of checkpoint activation impacted by Pch2 (see above), such as Hop1^{T318} phosphorylation, Mek1 hyperphosphorylation and histone H3T11 phosphorylation (Figure 8E). Consistent with the alleviation of meiotic arrest (Figure 8C and D), the high levels of phospho-Hop1^{T318} and Mek1 hyperactivation observed in *zip1* were drastically reduced in both *zip1 pch2-K320A* and *zip1 pch2-E399Q* double mutants (Figure 8E). Like in *zip1 pch2Δ*, *HOP1* overexpression restored Hop1^{T318} phosphorylation and Mek1 activation in both ATPase mutants (Supplementary Figure S5). Thus, both ATP binding to the Walker A motif and ATP hydrolysis by the Walker B module are critical for Pch2's meiotic checkpoint function.

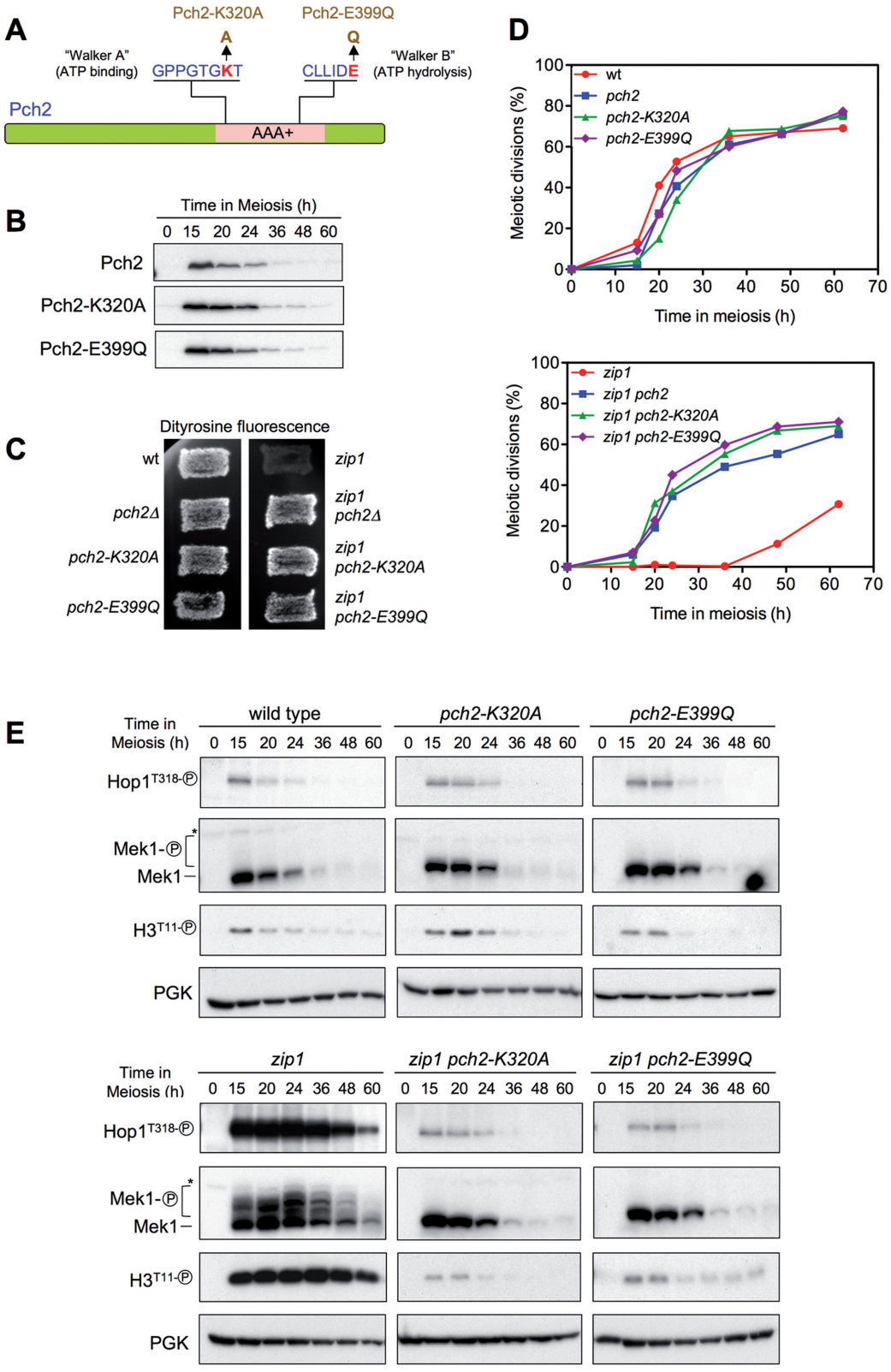

Figure 8. The ATPase activity of Pch2 is required for its checkpoint function. (**A**) Schematic representation of the Pch2 protein indicating the AAA+ domain, the conserved Walker A and Walker B motifs, and the mutations introduced at both sites. (**B**) Western blot analysis of Pch2, Pch2-K320A or Pch2-E399Q production (detected with anti-HA antibodies) during meiosis. (**C**) Dityrosine fluorescence assay. (**D**) Time course of meiotic nuclear divisions; the percentage of cells containing two or more nuclei is represented. (E) Western blot analysis of Hop1^{T318} phosphorylation and Mek1 activation. PGK was used as a loading control. Strains are: DP1151 (wild type), DP1164 (*pch2Δ*), DP1163 (*pch2-K320A*), DP1287 (*pch2-E399Q*), DP1152 (*zip1*), DP1161 (*zip1 pch2Δ*), DP1162 (*zip1 pch2-K320A*) and DP1288 (*zip1 pch2-E399Q*).

Table 1. Sporulation and spore viability

Genotype	Sporulation frequency (%)	Spore Viability (%)
Wild type	66.8	95.3
pch2Δ	73.9	90.7
pch2-K320A	64.6	96.5
pch2-E399Q	80.3	93.0
zip1	2.0	nd
zip1 pch2Δ	83.3	35.2
zip1 pch2-K320A	77.3	46.5
zip1 pch2-E399Q	80.3	31.2
Wild type + *OE-HOP1*	65.3	92.0
pch2Δ + *OE-HOP1*	20,3	94.4

Sporulation frequency and spore viability was determined as explained in Materials and Methods. nd, not determined.
OE-: overexpression.

ATP binding to Pch2 is required for its localization and complex stability

We also analyzed the localization of wild-type Pch2 and the ATPase-dead versions on pachytene chromosome spreads. As previously described, the wild-type Pch2 protein showed a conspicuous accumulation in a particular chromosomal region lacking Hop1 that corresponds to the rDNA array (18) (Figure 9Aa, Ad). In addition, faint foci outside the rDNA can be found on wild-type chromosomes displaying an exclusive localization with Hop1 (18,22) (Supplementary Figure S6, white arrows). Surprisingly, despite being present at normal levels in whole cell extracts (Figure 8B), the Walker A-deficient Pch2-K320A protein was not detectable at any location on meiotic chromosomes of either wild-type or *zip1* spread nuclei (Figure 9Ab and Ae). In contrast, the Pch2-E399Q protein showed normal rDNA localization (Figure 9Ac and Af) even though it is catalytically inactive (63) and lacks checkpoint function (Figure 8). Remarkably, like in *pch2Δ* (Figure 4Ab), the Hop1 protein was also more abundant on chromosomes and displayed a linear instead of a dotty pattern in both *pch2-K320A* and *pch2-E399Q* single mutants (Figure 9Ab and Ac). On the contrary, but also similar to *zip1 pch2Δ* (Figure 4Ad), Hop1 localization was disrupted and discontinuous in *zip1 pch2-K320A* and *zip1 pch2-E399Q* double mutants (Figure 9Ae and Af). In addition, the characteristic exclusion of Hop1 from the rDNA region (18,55) was lost in the ATPase-deficient mutants (Figure 9A; arrows); in fact, the Pch2-E399Q protein extensively colocalized with Hop1 at the rDNA (Figure 9Ac and Af). Moreover, in contrast to the wild type, chromosomal foci of Pch2-E399Q also colocalized with Hop1 (Supplementary Figure S6, yellow arrows).

Since the Pch2-K320A version was not associated to the meiotic chromatin, we next studied the subcellular localization of Pch2 and Pch2-K320A by immunofluorescence in whole meiotic *zip1* cells. The wild-type Pch2 was prominently detected in a discrete lateral nuclear region devoid of Hop1, presumably the nucleolus (Figure 9B, arrow). On the other hand, Pch2-K320A did not accumulate in the nucleus and was present rather evenly dispersed throughout the cell (Figure 9B). Interestingly, total cellular levels of Hop1 were higher in the *zip1 pch2-K320A* mutant (Figure 9B), although the protein was not massively incorporated onto the chromosome axes (Figure 9Ae).

Mutation of this conserved lysine in the Walker A motif of AAA+ family members commonly abolishes ATP binding and therefore ATPase activity *in vitro*, as has been demonstrated for Pch2 (63) but, in addition, it often leads to dissociation of the hexameric complex into monomers, as has been described for the HslU and SV40 LTag AAA+ ATPases (65). Therefore, we analyzed whether the *pch2-K320A* mutation compromises the formation of the Pch2 hexameric complex *in vivo*. We generated wild-type and *pch2-K320A* heterozygous diploid strains in which one copy of the *PCH2* (or *pch2-K320A*) gene was tagged with the HA epitope and the other copy with the Myc epitope (Figure 10). In the wild type (*PCH2-HA/PCH2-Myc*), the anti-HA antibody immunoprecipitated both Pch2-HA and Pch2-Myc, consistent with the formation of a stable complex. In contrast, the anti-HA antibody failed to immunoprecipitate the Myc-tagged subunits in the *pch2-K320A-HA/pch2-K320A-Myc* strain (Figure 10A), suggesting that ATP binding is required for the integrity or stability of the Pch2 hexameric ring *in vivo* (Figure 10B).

In summary, the ATPase activity of Pch2 is absolutely required for the checkpoint response to *zip1* meiotic defects and orchestrates proper Hop1 subcellular distribution, chromosomal localization and phosphorylation. ATP binding to the Walker A motif of Pch2, but not ATP hydrolysis, is essential for its nuclear accumulation and association to the meiotic chromosomes.

DISCUSSION

Suppression of *pch2* checkpoint defect by Hop1 overproduction

Previous studies have reported that the Pch2 protein is an important player in the meiotic checkpoint response triggered by the absence of Zip1, a major structural component of the central region of the synaptonemal complex. This work provides new insights into the role of Pch2 in this process; we show that the critical function of Pch2 in the *zip1*-induced checkpoint is to promote Mec1/Tel1-dependent Hop1 phosphorylation at T318 and, therefore, the ensuing Mek1 full activation leading to the meiotic cell cycle block. We also show here that the ATPase activity of Pch2 is essential for this checkpoint function.

We report the isolation of *HOP1* in a genetic screen for high-copy suppressors of the *pch2* checkpoint defect.

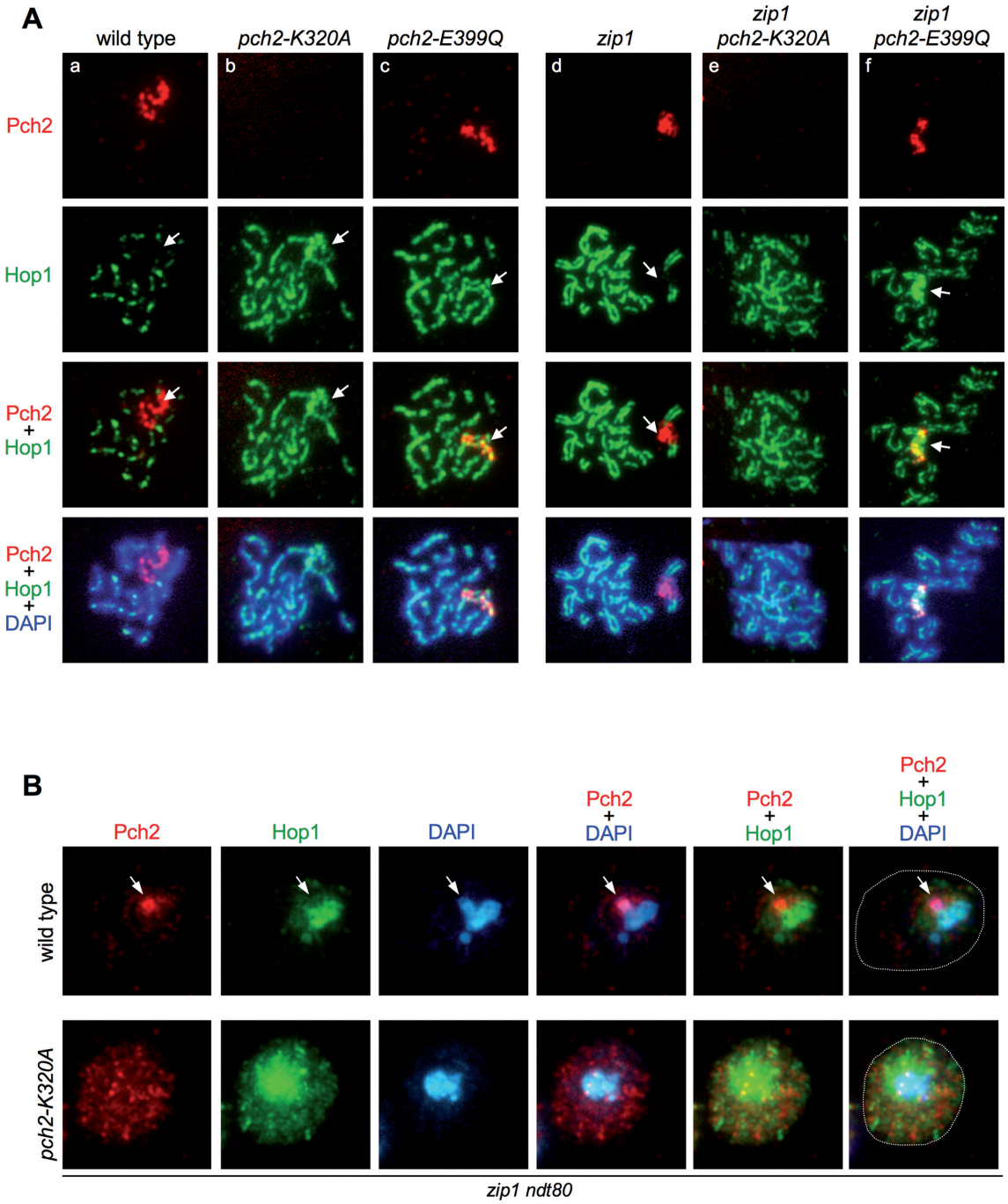

Figure 9. Localization of ATPase-deficient versions of Pch2. (**A**) Immunofluorescence of meiotic chromosomes stained with anti-HA or anti-MYC antibodies to detect Pch2, Pch2-K320A or Pch2-E399Q (red), anti-Hop1 antibodies (green) and DAPI (blue). Strains are: DP1243 (wild type), DP1193 (*pch2-K320A*), DP1262 (*pch2-E399Q*), DP1244 (*zip1*), DP1192 (*zip1 pch2-K320A*) and DP1263 (*zip1 pch2-E399Q*). (**B**) Immunofluorescence of whole meiotic cells stained with anti-HA antibodies (to detect Pch2 or Pch2-K320A; red), anti-Hop1 antibodies (green) and DAPI (blue). The contour of the cells is outlined in the rightmost panels. Representative cells 24 h after meiotic induction in *zip1 ndt80* background are shown. The arrows point to the rDNA region, which is distinguishable by the accumulation of Pch2 and the absence of Hop1. This region is not recognizable in the *pch2-K320A* mutant due to the mislocalization of Pch2-K320A and Hop1. Strains are: DP1190 (wild type) and DP1192 (*pch2-K320A*).

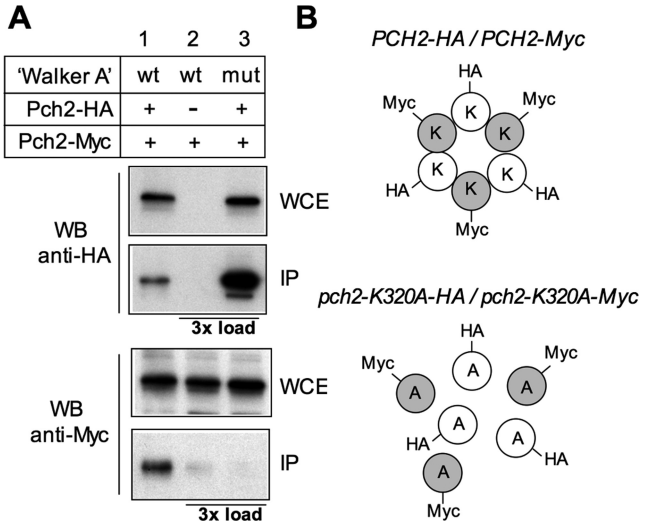

Figure 10. Mutation of the Pch2 ATP-binding site impairs the stability of the hexameric complex. (**A**) Whole cell extracts (WCE) prepared after 16 h in meiosis were immunoprecipitated with anti-HA antibodies. WCE and immunoprecipitates (IP) were analyzed by Western blot with both anti-HA and anti-Myc antibodies, as indicated. Strains are: DP1325 (*PCH2-HA/PCH2-Myc*; lane 1), DP1329 (*PCH2/PCH2-Myc*; lane 2) and DP1337 (*pch2-K320A-HA/pch2-K320A-Myc*; lane 3). To discard a problem with detection levels, in lane 2 (HA-untagged control) and lane 3, three more times of IP compared to lane 1 were loaded. (**B**) Schematic interpretation of the result described in (A). K and A represent a lysine and an alanine, respectively, at position 320 of Pch2.

Monitoring various cytological and molecular markers, we demonstrate that high levels of Hop1 restore checkpoint function in a *zip1 pch2* mutant restraining meiotic cell cycle progression. This finding was unanticipated, since it has been well established that Pch2 negatively regulates Hop1 abundance (at least on synapsed chromosomes) (18,21,22). Since Hop1 chromosomal levels are higher in the *pch2* mutant it was unexpected that additional amounts of Hop1 provided by an overexpression plasmid could suppress the phenotype resulting from the lack of Pch2. Nevertheless, the Hop1 remodeling function reported for Pch2 has been only analyzed in the context of synapsed chromosomes, where Pch2 determines an alternating pattern of Hop1 abundance (21) (Figure 11). We show here in the context of unsynapsed chromosomes that, although global cellular levels of Hop1 are higher in *zip1 pch2* compared with *zip1*, the extensive incorporation of Hop1 onto the lateral elements of *zip1* chromosomes is not further increased when *PCH2* is deleted. However, the rDNA region, normally devoid of Hop1, is decorated by the Hop1 protein in both *pch2* and *zip1 pch2* mutants, consistent with the nucleolar localization of Pch2 in both wild type and *zip1* nuclei. Notably, although Pch2 and Hop1 display largely exclusive localization patterns on wild-type chromosomes, we show that the catalytically-inactive Pch2-E399Q protein colocalizes with Hop1 both at chromosomal foci and the rDNA confirming that the ATPase activity of Pch2 is required for displacing Hop1 from the meiotic chromatin *in vivo* like it does *in vitro* (63).

Regulation of Hop1 phosphorylation

Phosphorylation of Hop1 at T318 by the Mec1/Tel1 checkpoint kinases is a requisite for Mek1 autophosphorylation and, therefore, for checkpoint activity. We show here that *zip1*-induced Hop1-T318 phosphorylation is drastically reduced in the absence of Pch2 or in ATPase-dead *pch2* mutants. This reduction is manifested both globally using western blot analysis of whole cell extracts and locally on chromosome spreads, indicating a general requirement for Pch2 to maintain high levels of Hop1-T318 phosphorylation when synapsis defects occur. The fact that overexpression of wild-type *HOP1*, but not that of a *hop1-T318A* mutant, restores the checkpoint in *zip1 pch2* reveals Hop1-T318 phosphorylation as the relevant target of Pch2's checkpoint function. Notably, although *HOP1* overexpression in the wild type has only minimal effects, it reduces sporulation efficiency in the *pch2* single mutant (Table 1), suggesting that Pch2 activity is required to maintain the proper balance of Hop1 abundance and phosphorylation also in the presence of synapsed chromosomes. We also note that Zip1 may contribute to the accumulation of phospho-Hop1^{T318} in *pch2* mutant chromosomes.

We show that meiotic defects persist in *zip1 pch2*; thus, in principle, two possibilities can be envisaged to explain the regulation of Hop1-T318 phosphorylation by the Pch2 ATPase: Pch2 might favor the action of the Mec1/Tel1 kinases on Hop1-T318 or, alternatively, may inhibit phospho-Hop1-T318 phosphatase(s). In line with the first option, Pch2 (together with Xrs2) promotes Tel1-dependent Hop1 phosphorylation in response to unresected DSBs in a *rad50S* mutant (29). However, Tel1 is not required for the *zip1*-induced synapsis checkpoint (29) pointing to a Tel1-independent function for Pch2 in this particular scenario. We also show here that the absence of Pch2 does not alter the localization of the Mec1-Ddc2 complex suggesting that Pch2 is not required for global Mec1 activity. Nevertheless, a local requirement for Pch2 in facilitating the access of Mec1 to the Hop1-T318 substrate on chromosome axes cannot be ruled out. In this scenario, Pch2's ATPase activity could be required to induce some conformational change in the vicinity of Hop1 enabling its phosphorylation at T318 by Mec1. The interaction of Red1 with SUMO chains promotes Hop1-T318 phosphorylation (66). It is possible that Pch2 differentially modulates this interaction in response to SC defects. In line with this possibility, a role for Pch2 in orchestrating the interdependence between Hop1 and Red1 for Hop1 phosphorylation has been proposed (67). Nevertheless, these studies have not been performed under checkpoint-inducing conditions (i.e. *zip1* mutant) where Pch2 may have different and/or additional functions (see below).

On the other hand, if Pch2 negatively regulates the phosphatase(s) involved in removing the phosphorylation of Hop1-T318, the lack of this phosphatase should reestablish the meiotic block in a *zip1 pch2* mutant. It has been proposed that PP4 is the main phosphatase reversing Hop1-T318 phosphorylation (7); therefore, we investigated the impact of PP4 in the response to *zip1* defects. In the BR1919 genetic background used in this study, the *zip1* mutant shows a checkpoint-induced meiotic block in prophase, but

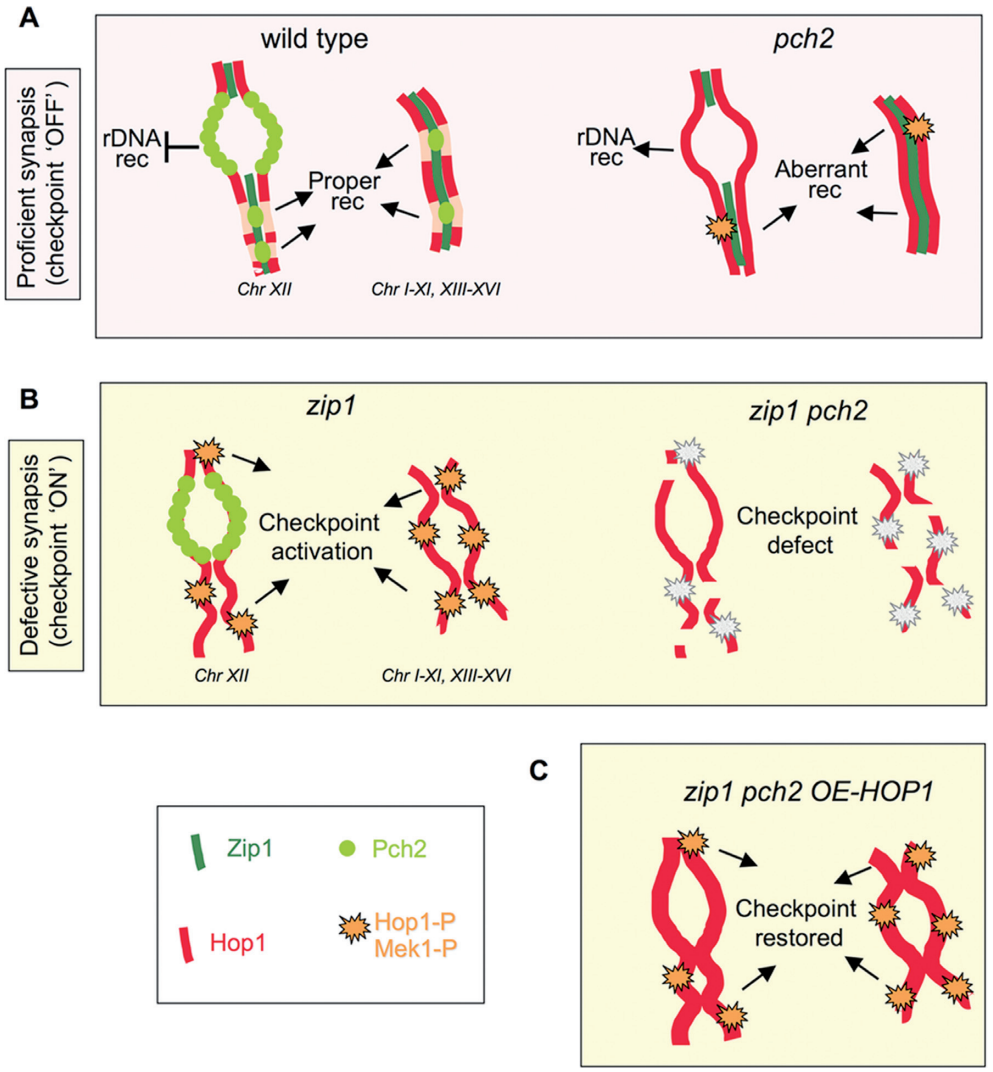

Figure 11. A model for Pch2 checkpoint function. (**A**) In unperturbed wild-type meiosis, nucleolar Pch2 excludes Hop1 from the rDNA preventing recombination at this chromosome XII array. In turn, chromosomal Pch2 dictates Hop1 discontinuous axis distribution sustaining proper synapsis and recombination. In the *pch2* single mutant, Hop1 localizes to the nucleolar region and unwanted rDNA recombination occurs. Hop1 is also more abundant on chromosome axes disturbing normal recombination events that slightly increase Hop1-T318 phosphorylation. Nevertheless, most recombination defects of the *pch2* mutant are only evident when DSBs are limiting (28,56). (**B**) In the synapsis-deficient *zip1* mutant, Pch2 is absent from the chromosomes and concentrated in the rDNA. This configuration supports continuous distribution of Hop1 along unsynapsed axes and high levels of Hop1-T318 phosphorylation relaying the checkpoint signal to Mek1 activation. When *PCH2* is deleted (or the ATPase inactivated), Hop1 loading and phosphorylation is impaired leading to inoperative checkpoint. (**C**) Despite the weakened Hop1/Mek1 activation, *HOP1* overexpression in *zip1 pch2* provides enough protein to restore high levels of global Hop1 phosphorylation and reinstate checkpoint function (see text for additional details).

at later time points at least a fraction of the cells resume cell cycle progression and complete the meiotic divisions. At the molecular level this meiotic resumption is manifested by an eventual decrease in Hop1-T318 phosphorylation and reduced Mek1 signaling (Figure 6). We found that the *zip1 pph3* double mutant displays more persistent Mek1 activation and a tighter meiotic block arguing that, indeed, PP4 is crucial for deactivation and/or adaptation of the *zip1*-induced checkpoint. However, we have observed that the absence of PP4 function only confers a partial restoration of Hop1-T318 phosphorylation in *zip1 pch2*, indicating that Pch2 does not primarily act on this phosphatase or that PP4 may not be the only phosphatase capable of dephosphorylating Hop1-T318. The simplest interpretation of this result is that the low levels of Hop1-T318 phosphorylation in *zip1 pch2*, perhaps resulting from crippled Mec1/Tel1 function, are increased to some extent when the inhibitory action of PP4 is removed. Regardless of the identity of the direct target of Pch2, these observations confirm that the crucial role of Pch2 in the *zip1* checkpoint is the fine regulation of Hop1-T318 phosphorylation status. In fact, these experiments reveal that manipulation of Hop1 phosphorylation in *zip1 pch2* by other means, such as deleting *PPH3*, but without altering *HOP1* expression levels also has an impact on the checkpoint.

Relevance of the ATPase activity for Pch2 checkpoint function

Recent *in vitro* analyses of the *S. cerevisiae* Pch2 protein have elegantly demonstrated that Pch2 is indeed an AAA+ ATPase that assembles into hexameric rings in the presence of nucleotides (63). That study also assessed the *in vivo* meiotic impact of mutations in the ATPase domain of Pch2 by determining the decrease in spore viability resulting from combining a *csm4* mutant with the loss of Pch2 function. However, since Csm4 is involved in chromosome movement during prophase driven by telomere attachment to the nuclear envelope (68–70) and there are multiple meiotic processes influenced by Pch2, the physiological basis of this synthetic spore viability defect with *csm4* is not obvious. Therefore, we analyzed the contribution of the ATPase activity to the well-established Pch2 role in the *zip1*-induced checkpoint. In contrast to the intermediate phenotype reported for the *pch2-K320A* mutant based on its combination with *csm4* (63), we show here that mutants defective in either ATP binding site (*pch2-K320A*) or ATP hydrolysis (*pch2-E399Q*) phenocopy the *pch2* deletion mutant for the checkpoint defect indicating that both activities are absolutely required for Pch2 checkpoint function. However, we observe a striking difference between both catalytically-inactive proteins in terms of localization on meiotic chromosome spreads. Whereas Pch2-E399Q displays the normal accumulation at the rDNA region on chromosome XII and some fainter interstitial chromosomal foci, the Pch2-K320A version completely fails to bind to the chromosomes. We found that the Pch2-K320A mutation preventing ATP binding compromises the integrity of the hexameric ring; this observation could explain the defect in localization, which may require an intact complex for its correct targeting. On the other hand, Pch2-E399Q does localize like the wild-type Pch2 protein; however, in contrast to Pch2, which does not overlap with Hop1 staining, the Pch2-E399Q version displays extensive colocalization with Hop1 both at chromosomal foci (in otherwise wild-type strains) and the rDNA, where Hop1 fails to be excluded in this mutant. These observations are consistent with the notion that Pch2/Trip13 utilizes the forces generated from ATP hydrolysis to displace or reorganize HORMA domain proteins, such as Hop1/HORMAD1 in meiosis or MAD2 in the SAC response (71). The effect of mammalian Trip13 on the conformational change of MAD2 is exerted with the help of the p31 adaptor (35). To determine whether yeast Pch2 requires additional cofactors or adaptors to disassemble Hop1 from meiotic chromosomes awaits further investigation. Nevertheless, *in vitro* assays show that purified Pch2 can directly alter Hop1 DNA binding properties (63).

A dual role for Pch2 on Hop1 regulation?

The Pch2 protein is predominantly found in the unsynapsed region of chromosome XII, which lacks Zip1 and Hop1, preventing recombination within the rDNA array (18,26). In addition, Pch2 is also present in SC-associated chromosomal foci promoting an alternating pattern of Zip1 and Hop1 during SC development (21). Curiously, whereas in yeast SK1 strains Pch2 chromosomal foci are conspicuous (22), in the BR strains used in this work, most Pch2 is detected in the nucleolar area with SC-associated foci showing a much weaker staining ((18); Figure 9 and Supplementary Figure S6). Importantly, in the synapsis-deficient *zip1* mutant, the chromosomal Pch2 protein is no longer detectable and it is exclusively observed in the rDNA ((18); Figure 9). These observations suggest that two populations of Pch2 with different requirements for chromosome binding may exist: the nucleolar Pch2 pool, which does not require Zip1 for being targeted to the unsynapsed rDNA array and the interstitial chromosomal Pch2 protein, which is likely dependent on Zip1 assembly for its localization. Both pools of Pch2 possess the ability to displace Hop1 from the chromosome axes because Hop1 is more abundant along the SC and accumulates in the rDNA region in *pch2* mutants lacking ATPase activity. However, since Pch2 function is critically required for the *zip1*-induced meiotic arrest, the fact that in the *zip1* mutant Pch2 is only present at the rDNA location implies that the nucleolar Pch2 protein is responsible for the checkpoint function by sustaining high levels of Hop1-T318 phosphorylation in response to synapsis defects (Figure 11).

How can Pch2 control Hop1 phosphorylation from the nucleolus where, precisely, Hop1 is excluded? A role for nucleolar proteins in the control of cell cycle events is a well-documented phenomenon (72). Perhaps, the most paradigmatic example is the regulation of mitotic exit in budding yeast by the FEAR/MEN pathways orchestrating the release of the Cdc14 phosphatase from the nucleolus during anaphase (73–75). In a similar scenario it is possible that, when synapsis is defective, Pch2 traps in the nucleolus a crucial regulator required for exit from pachytene. Upon synapsis completion this factor would be released promoting entry into meiosis I. The PP4 phosphatase was a good candidate to meet these requirements because it promotes Hop1-T318 dephosphorylation and, hence, checkpoint inactivation, but our results indicate that Pch2 does not primarily acts via PP4 regulation (see above). In addition, during meiotic prophase PP4 appears to be localized at centromeres, not the nucleolus (76). We have also tested another phosphatase, PP1, which displays nucleolar localization at least during some stages of the cell cycle (77). In contrast to a previous study reporting a role for Glc7 -the catalytic subunit of PP1- in reversing Mek1 activation (38), we have found a minimal, if any, effect of either a *glc7-T152K* allele or a meiotic-depletion *glc7-md* mutant in Hop1 or Mek1 phosphorylation, and no evidence of functional relationship between Glc7 and Pch2 (AL and PSS, unpublished results). Alternatively, nucleolar Pch2 could control the localization of a Mec1 activator in response to synapsis defects. Since the N-terminal domain of Xrs2 physically interacts with Pch2 (29), it will be interesting to further investigate how this interaction impinges on Hop1 regulation in response to SC defects.

In sum, our results are consistent with a differential regulation of Hop1 by chromosomal and nucleolar Pch2 in a wild-type (checkpoint OFF) versus a *zip1* (checkpoint ON) situation (Figure 11). The identification of Pch2 co-factors that may modulate its action on Hop1 depending on the specific chromosomal context or synapsis status will help to elucidate the basis of this differential effect.

SUPPLEMENTARY DATA

Supplementary Data are available at NAR Online.

ACKNOWLEDGEMENTS

The authors are grateful to Rodrigo Bermejo for a *pph3Δ* strain, Félix Prado for *delitto perfetto* reagents, Jesús Carballo for the phospho-Hop1-T318 antibody, Olga Calvo for the anti-GFP antibody, and Amy MacQueen and Shirleen Roeder for plasmids and strains. We also thank Vanessa Silva Dutra de Carvalho for help with some experiments, Isabel Acosta for technical assistance and Jesús Carballo and Andrés Clemente for helpful discussions and ideas.

FUNDING

Ministry of Economy and Competitiveness (MINECO) of Spain [BFU2012-35748 and BFU2015-65417-R]; Predoctoral contract from the University of Salamanca (Spain) (to E.H.); Predoctoral fellowship (JAE-predoc) (to D.O.) and a postdoctoral fellowship (JAE-doc) (to S.C.) from the CSIC (Spain). Funding for open access charge: Ministry of Economy and Competitiveness (MINECO) of Spain [BFU2012-35748 and BFU2015-65417-R].
Conflict of interest statement. None declared.

REFERENCES

1. MacQueen,A.J. and Hochwagen,A. (2011) Checkpoint mechanisms: the puppet masters of meiotic prophase. *Trends Cell. Biol.*, **21**, 393–400.
2. Roeder,G.S. and Bailis,J.M. (2000) The pachytene checkpoint. *Trends Genet.*, **16**, 395–403.
3. Subramanian,V.V. and Hochwagen,A. (2014) The meiotic checkpoint network: step-by-step through Meiotic Prophase. *Cold Spring Harb. Perspect. Biol.*, **6**, e1002369.
4. Schwacha,A. and Kleckner,N. (1997) Interhomolog bias during meiotic recombination: meiotic functions promote a highly differentiated interhomolog-only pathway. *Cell*, **90**, 1123–1135.
5. Sym,M., Engebrecht,J.A. and Roeder,G.S. (1993) ZIP1 is a synaptonemal complex protein required for meiotic chromosome synapsis. *Cell*, **72**, 365–378.
6. Carballo,J.A., Johnson,A.L., Sedgwick,S.G. and Cha,R.S. (2008) Phosphorylation of the axial element protein Hop1 by Mec1/Tel1 ensures meiotic interhomolog recombination. *Cell*, **132**, 758–770.
7. Chuang,C.N., Cheng,Y.H. and Wang,T.F. (2012) Mek1 stabilizes Hop1-Thr318 phosphorylation to promote interhomolog recombination and checkpoint responses during yeast meiosis. *Nucleic Acids Res.*, **40**, 11416–11427.
8. Ontoso,D., Acosta,I., van Leeuwen,F., Freire,R. and San-Segundo,P.A. (2013) Dot1-dependent histone H3K79 methylation promotes activation of the Mek1 meiotic checkpoint effector kinase by regulating the Hop1 adaptor. *PLoS Genet.*, **9**, e1003262.
9. Niu,H., Li,X., Job,E., Park,C., Moazed,D., Gygi,S.P. and Hollingsworth,N.M. (2007) Mek1 kinase is regulated to suppress double-strand break repair between sister chromatids during budding yeast meiosis. *Mol. Cell. Biol.*, **27**, 5456–5467.
10. Niu,H., Wan,L., Baumgartner,B., Schaefer,D., Loidl,J. and Hollingsworth,N.M. (2005) Partner choice during meiosis is regulated by Hop1-promoted dimerization of Mek1. *Mol. Biol. Cell*, **16**, 5804–5818.
11. Terentyev,Y., Johnson,R., Neale,M.J., Khisroon,M., Bishop-Bailey,A. and Goldman,A.S. (2010) Evidence that MEK1 positively promotes interhomologue double-strand break repair. *Nucleic Acids Res.*, **38**, 4349–4360.
12. Niu,H., Wan,L., Busygina,V., Kwon,Y., Allen,J.A., Li,X., Kunz,R.C., Kubota,K., Wang,B., Sung,P. *et al.* (2009) Regulation of meiotic recombination via Mek1-mediated Rad54 phosphorylation. *Mol. Cell*, **36**, 393–404.
13. Acosta,I., Ontoso,D. and San-Segundo,P.A. (2011) The budding yeast polo-like kinase Cdc5 regulates the Ndt80 branch of the meiotic recombination checkpoint pathway. *Mol. Biol. Cell*, **22**, 3478–3490.
14. Leu,J.Y. and Roeder,G.S. (1999) The pachytene checkpoint in *S. cerevisiae* depends on Swe1-mediated phosphorylation of the cyclin-dependent kinase Cdc28. *Mol. Cell*, **4**, 805–814.
15. Tung,K.S., Hong,E.J. and Roeder,G.S. (2000) The pachytene checkpoint prevents accumulation and phosphorylation of the meiosis-specific transcription factor Ndt80. *Proc. Natl. Acad. Sci. U.S.A.*, **97**, 12187–12192.
16. Wang,Y., Chang,C.Y., Wu,J.F. and Tung,K.S. (2011) Nuclear localization of the meiosis-specific transcription factor Ndt80 is regulated by the pachytene checkpoint. *Mol. Biol. Cell*, **22**, 1878–1886.
17. Eichinger,C.S. and Jentsch,S. (2010) Synaptonemal complex formation and meiotic checkpoint signaling are linked to the lateral element protein Red1. *Proc. Natl. Acad. Sci. U.S.A.*, **107**, 11370–11375.
18. San-Segundo,P.A. and Roeder,G.S. (1999) Pch2 links chromatin silencing to meiotic checkpoint control. *Cell*, **97**, 313–324.
19. San-Segundo,P.A. and Roeder,G.S. (2000) Role for the silencing protein Dot1 in meiotic checkpoint control. *Mol. Biol. Cell*, **11**, 3601–3615.
20. Wu,H.Y. and Burgess,S.M. (2006) Two distinct surveillance mechanisms monitor meiotic chromosome metabolism in budding yeast. *Curr. Biol.*, **16**, 2473–2479.
21. Borner,G.V., Barot,A. and Kleckner,N. (2008) Yeast Pch2 promotes domainal axis organization, timely recombination progression, and arrest of defective recombinosomes during meiosis. *Proc. Natl. Acad. Sci. U.S.A.*, **105**, 3327–3332.
22. Joshi,N., Barot,A., Jamison,C. and Borner,G.V. (2009) Pch2 links chromosome axis remodeling at future crossover sites and crossover distribution during yeast meiosis. *PLoS Genet.*, **5**, e1000557.
23. Wojtasz,L., Daniel,K., Roig,I., Bolcun-Filas,E., Xu,H., Boonsanay,V., Eckmann,C.R., Cooke,H.J., Jasin,M., Keeney,S. *et al.* (2009) Mouse HORMAD1 and HORMAD2, two conserved meiotic chromosomal proteins, are depleted from synapsed chromosome axes with the help of TRIP13 AAA-ATPase. *PLoS Genet.*, **5**, e1000702.
24. Farmer,S., Hong,E.J., Leung,W.K., Argunhan,B., Terentyev,Y., Humphryes,N., Toyoizumi,H. and Tsubouchi,H. (2012) Budding yeast Pch2, a widely conserved meiotic protein, is involved in the initiation of meiotic recombination. *PLoS One*, **7**, e39724.
25. Roig,I., Dowdle,J.A., Toth,A., de Rooij,D.G., Jasin,M. and Keeney,S. (2010) Mouse TRIP13/PCH2 is required for recombination and normal higher-order chromosome structure during meiosis. *PLoS Genet.*, **6**, e1001062.
26. Vader,G., Blitzblau,H.G., Tame,M.A., Falk,J.E., Curtin,L. and Hochwagen,A. (2011) Protection of repetitive DNA borders from self-induced meiotic instability. *Nature*, **477**, 115–119.
27. Zanders,S. and Alani,E. (2009) The *pch2Δ*; mutation in baker's yeast alters meiotic crossover levels and confers a defect in crossover interference. *PLoS Genet.*, **5**, e1000571.
28. Zanders,S., Sonntag Brown,M., Chen,C. and Alani,E. (2011) Pch2 modulates chromatid partner choice during meiotic double-strand break repair in *Saccharomyces cerevisiae*. *Genetics*, **188**, 511–521.
29. Ho,H.C. and Burgess,S.M. (2011) Pch2 acts through Xrs2 and Tel1/ATM to modulate interhomolog bias and checkpoint function during meiosis. *PLoS Genet.*, **7**, e1002351.
30. Eytan,E., Wang,K., Miniowitz-Shemtov,S., Sitry-Shevah,D., Kaisari,S., Yen,T.J., Liu,S.T. and Hershko,A. (2014) Disassembly of mitotic checkpoint complexes by the joint action of the AAA-ATPase TRIP13 and p31(comet). *Proc. Natl. Acad. Sci. U.S.A.*, **111**, 12019–12024.
31. Nelson,C.R., Hwang,T., Chen,P.H. and Bhalla,N. (2015) TRIP13^{PCH-2} promotes Mad2 localization to unattached kinetochores in the spindle checkpoint response. *J. Cell Biol.*, **211**, 503–516.
32. Wang,K., Sturt-Gillespie,B., Hittle,J.C., Macdonald,D., Chan,G.K., Yen,T.J. and Liu,S.T. (2014) Thyroid hormone receptor interacting protein 13 (TRIP13) AAA-ATPase is a novel mitotic checkpoint-silencing protein. *J. Biol. Chem.*, **289**, 23928–23937.

33. Banerjee,R., Russo,N., Liu,M., Basrur,V., Bellile,E., Palanisamy,N., Scanlon,C.S., van Tubergen,E., Inglehart,R.C., Metwally,T. *et al.* (2014) TRIP13 promotes error-prone nonhomologous end joining and induces chemoresistance in head and neck cancer. *Nat. Commun.*, **5**, 4527.
34. Martin,K.J., Patrick,D.R., Bissell,M.J. and Fournier,M.V. (2008) Prognostic breast cancer signature identified from 3D culture model accurately predicts clinical outcome across independent datasets. *PLoS One*, **3**, e2994.
35. Ye,Q., Rosenberg,S.C., Moeller,A., Speir,J.A., Su,T.Y. and Corbett,K.D. (2015) TRIP13 is a protein-remodeling AAA+ ATPase that catalyzes MAD2 conformation switching. *Elife*, **4**, e07367.
36. Rockmill,B. and Roeder,G.S. (1990) Meiosis in asynaptic yeast. *Genetics*, **126**, 563–574.
37. Agarwal,S. and Roeder,G.S. (2000) Zip3 provides a link between recombination enzymes and synaptonemal complex proteins. *Cell*, **102**, 245–255.
38. Bailis,J.M. and Roeder,G.S. (2000) Pachytene exit controlled by reversal of Mek1-dependent phosphorylation. *Cell*, **101**, 211–221.
39. Humphryes,N., Leung,W.K., Argunhan,B., Terentyev,Y., Dvorackova,M. and Tsubouchi,H. (2013) The Ecm11-Gmc2 complex promotes synaptonemal complex formation through assembly of transverse filaments in budding yeast. *PLoS Genet.*, **9**, e1003194.
40. Goldstein,A.L. and McCusker,J.H. (1999) Three new dominant drug resistance cassettes for gene disruption in *Saccharomyces cerevisiae*. *Yeast*, **15**, 1541–1553.
41. Voth,W.P., Jiang,Y.W. and Stillman,D.J. (2003) New 'marker swap' plasmids for converting selectable markers on budding yeast gene disruptions and plasmids. *Yeast*, **20**, 985–993.
42. Schneider,B.L., Seufert,W., Steiner,B., Yang,Q.H. and Futcher,A.B. (1995) Use of polymerase chain reaction epitope tagging for protein tagging in *Saccharomyces cerevisiae*. *Yeast*, **11**, 1265–1274.
43. Refolio,E., Cavero,S., Marcon,E., Freire,R. and San-Segundo,P.A. (2011) The Ddc2/ATRIP checkpoint protein monitors meiotic recombination intermediates. *J. Cell Sci.*, **124**, 2488–2500.
44. Stuckey,S., Mukherjee,K. and Storici,F. (2011) In vivo site-specific mutagenesis and gene collage using the delitto perfetto system in yeast *Saccharomyces cerevisiae*. *Methods Mol. Biol.*, **745**, 173–191.
45. Hollingsworth,N.M. and Ponte,L. (1997) Genetic interactions between *HOP1*, *RED1* and *MEK1* suggest that *MEK1* regulates assembly of axial element components during meiosis in the yeast *Saccharomyces cerevisiae*. *Genetics*, **147**, 33–42.
46. Carlson,M. and Botstein,D. (1982) Two differentially regulated mRNAs with different 5′ ends encode secreted with intracellular forms of yeast invertase. *Cell*, **28**, 145–154.
47. Rockmill,B. (2009) Chromosome spreading and immunofluorescence methods in *Saccharomyes cerevisiae*. *Methods Mol. Biol.*, **558**, 3–13.
48. Santos,B., Duran,A. and Valdivieso,M.H. (1997) *CHS5*, a gene involved in chitin synthesis and mating in *Saccharomyces cerevisiae*. *Mol. Cell. Biol.*, **17**, 2485–2496.
49. Xu,L., Ajimura,M., Padmore,R., Klein,C. and Kleckner,N. (1995) NDT80, a meiosis-specific gene required for exit from pachytene in *Saccharomyces cerevisiae*. *Mol. Cell. Biol.*, **15**, 6572–6581.
50. Collart,M.A. (1996) The *NOT*, *SPT3*, and *MOT1* genes functionally interact to regulate transcription at core promoters. *Mol. Cell. Biol.*, **16**, 6668–6676.
51. Lydall,D., Nikolsky,Y., Bishop,D.K. and Weinert,T. (1996) A meiotic recombination checkpoint controlled by mitotic checkpoint genes. *Nature*, **383**, 840–843.
52. Majka,J. and Burgers,P.M. (2007) Clamping the Mec1/ATR checkpoint kinase into action. *Cell Cycle*, **6**, 1157–1160.
53. Hong,E.J. and Roeder,G.S. (2002) A role for Ddc1 in signaling meiotic double-strand breaks at the pachytene checkpoint. *Genes Dev.*, **16**, 363–376.
54. Govin,J., Dorsey,J., Gaucher,J., Rousseaux,S., Khochbin,S. and Berger,S.L. (2010) Systematic screen reveals new functional dynamics of histones H3 and H4 during gametogenesis. *Genes Dev.*, **24**, 1772–1786.
55. Smith,A.V. and Roeder,G.S. (1997) The yeast Red1 protein localizes to the cores of meiotic chromosomes. *J. Cell Biol.*, **136**, 957–967.
56. Joshi,N., Brown,M.S., Bishop,D.K. and Borner,G.V. (2015) Gradual implementation of the meiotic recombination program via checkpoint pathways controlled by global DSB levels. *Mol. Cell*, **57**, 797–811.
57. Arbel,A., Zenvirth,D. and Simchen,G. (1999) Sister chromatid-based DNA repair is mediated by RAD54, not by DMC1 or TID1. *EMBO J.*, **18**, 2648–2658.
58. Liu,Y., Gaines,W.A., Callender,T., Busygina,V., Oke,A., Sung,P., Fung,J.C. and Hollingsworth,N.M. (2014) Down-regulation of Rad51 activity during meiosis in yeast prevents competition with Dmc1 for repair of double-strand breaks. *PLoS Genet.*, **10**, e1004005.
59. Raschle,M., Van Komen,S., Chi,P., Ellenberger,T. and Sung,P. (2004) Multiple interactions with the Rad51 recombinase govern the homologous recombination function of Rad54. *J. Biol. Chem.*, **279**, 51973–51980.
60. Cheng,C.H., Lo,Y.H., Liang,S.S., Ti,S.C., Lin,F.M., Yeh,C.H., Huang,H.Y. and Wang,T.F. (2006) SUMO modifications control assembly of synaptonemal complex and polycomplex in meiosis of *Saccharomyces cerevisiae*. *Genes Dev.*, **20**, 2067–2081.
61. Lynn,A., Soucek,R. and Borner,G.V. (2007) ZMM proteins during meiosis: crossover artists at work. *Chromosome Res.*, **15**, 591–605.
62. Voelkel-Meiman,K., Taylor,L.F., Mukherjee,P., Humphryes,N., Tsubouchi,H. and Macqueen,A.J. (2013) SUMO localizes to the central element of synaptonemal complex and is required for the full synapsis of meiotic chromosomes in budding yeast. *PLoS Genet.*, **9**, e1003837.
63. Chen,C., Jomaa,A., Ortega,J. and Alani,E.E. (2014) Pch2 is a hexameric ring ATPase that remodels the chromosome axis protein Hop1. *Proc. Natl. Acad. Sci. U.S.A.*, **111**, E44–E53.
64. Hanson,P.I. and Whiteheart,S.W. (2005) AAA+ proteins: have engine, will work. *Nat. Rev. Mol. Cell. Biol.*, **6**, 519–529.
65. Wendler,P., Ciniawsky,S., Kock,M. and Kube,S. (2012) Structure and function of the AAA+ nucleotide binding pocket. *Biochim. Biophys. Acta*, **1823**, 2–14.
66. Lin,F.M., Lai,Y.J., Shen,H.J., Cheng,Y.H. and Wang,T.F. (2010) Yeast axial-element protein, Red1, binds SUMO chains to promote meiotic interhomologue recombination and chromosome synapsis. *EMBO J.*, **29**, 586–596.
67. Lo,Y.H., Chuang,C.N. and Wang,T.F. (2014) Pch2 prevents Mec1/Tel1-mediated Hop1 phosphorylation occurring independently of Red1 in budding yeast meiosis. *PLoS One*, **9**, e85687.
68. Conrad,M.N., Lee,C.Y., Chao,G., Shinohara,M., Kosaka,H., Shinohara,A., Conchello,J.A. and Dresser,M.E. (2008) Rapid telomere movement in meiotic prophase is promoted by NDJ1, MPS3, and CSM4 and is modulated by recombination. *Cell*, **133**, 1175–1187.
69. Kosaka,H., Shinohara,M. and Shinohara,A. (2008) Csm4-dependent telomere movement on nuclear envelope promotes meiotic recombination. *PLoS Genet.*, **4**, e1000196.
70. Wanat,J.J., Kim,K.P., Koszul,R., Zanders,S., Weiner,B., Kleckner,N. and Alani,E. (2008) Csm4, in collaboration with Ndj1, mediates telomere-led chromosome dynamics and recombination during yeast meiosis. *PLoS Genet.*, **4**, e1000188.
71. Vader,G. (2015) Pch2(TRIP13): controlling cell division through regulation of HORMA domains. *Chromosoma*, **124**, 333–339.
72. Pederson,T. (2011) The nucleolus. *Cold Spring Harb. Perspect. Biol.*, **3**, a000638.
73. Shou,W., Seol,J.H., Shevchenko,A., Baskerville,C., Moazed,D., Chen,Z.W., Jang,J., Charbonneau,H. and Deshaies,R.J. (1999) Exit from mitosis is triggered by Tem1-dependent release of the protein phosphatase Cdc14 from nucleolar RENT complex. *Cell*, **97**, 233–244.
74. Stegmeier,F., Visintin,R. and Amon,A. (2002) Separase, polo kinase, the kinetochore protein Slk19, and Spo12 function in a network that controls Cdc14 localization during early anaphase. *Cell*, **108**, 207–220.
75. Visintin,R., Hwang,E.S. and Amon,A. (1999) Cfi1 prevents premature exit from mitosis by anchoring Cdc14 phosphatase in the nucleolus. *Nature*, **398**, 818–823.
76. Falk,J.E., Chan,A.C., Hoffmann,E. and Hochwagen,A. (2010) A Mec1- and PP4-dependent checkpoint couples centromere pairing to meiotic recombination. *Dev. Cell*, **19**, 599–611.
77. Bloecher,A. and Tatchell,K. (2000) Dynamic localization of protein phosphatase type 1 in the mitotic cell cycle of *Saccharomyces cerevisiae*. *J. Cell Biol.*, **149**, 125–140.